DEUTSCHES ELEKTRONEN-SYNCHROTRON DESY

DESY 80/45
May 1980

PHENOMENOLOGY OF JETS

by

T. F. Walsh

NOTKESTRASSE 85 · 2 HAMBURG 52

To be sure that your preprints are promptly included in the
HIGH ENERGY PHYSICS INDEX ,
send them to the following address (if possible by air mail) :

DESY
Bibliothek
Notkestrasse 85
2 Hamburg 52
Germany

DESY 80/45
May 1980

Phenomenology of Jets

T. F. Walsh

XIX Internationale Universitätswochen
für Kernphysik

Schladming, Austria, Feb. 20-29, 1980

The basic idea of these lectures is very simple. Quarks and gluons - the elementary quanta of quantum chromodynamics or QCD - are produced with perturbatively calculable rates in short distance processes. This is because of asymptotic freedom! These quanta produced at short distances are, in a sense, "visible" as jets of hadrons. (The jets do not contain the colored QCD quanta if - as we will assume - color is confined. The jets contain only colorless hadrons.) The distribution of these jets is the distribution of the original quanta, apart from fluctuations generated in the (long distance) jet formation process. The distribution of the jets can thus test QCD in a particularly clear way at the parton level, at distances of order 5×10^{-16} cm (PETRA/PEP energies). Topics are

I. Confinement Jet Notions

II. Perturbative QCD tests

A) $Q\bar{Q} \rightarrow 3G$

B) $e^+e^- \rightarrow q\bar{q} + q\bar{q}G \rightarrow 2$ Jets + 3 Jets

III. Gluon Jets

IV. QCD Multijet Structure at High Energy

Lack of time and wisdom dictate the rather narrow focus on e^+e^- initiated short-distance reactions.

I. Confinement Jet Notions

1. Minimal Confinement Mythology

Unfortunately, most of what we know about confinement effects on short distance QCD tests are empirical observations strung together and rationalized as myth. Little of it is derived from first principles. Nevertheless, the myth is respectable. It may be useful to start with the space-time picture of deep inelastic processes[2]. Consider lepton-pion scattering, as the simplest example. At rest a pion probed by long wavelength photons is just a charged glob. At very large $\ell\pi$ center of mass energy and very large Q^2 (the Bjorken limit $x = Q^2/2P_\pi\cdot(p_\ell - p_{\ell'})$ fixed as $Q^2 \to \infty$) the pion is Lorentz contracted and probed at distances $O(1/\sqrt{Q^2})$. Fig. 1 shows what it looks like in a two dimensional Minkowski plot. At times and distances of order $1/\sqrt{Q^2}$ (when the deep inelastic reaction takes place) the pion is q, $\bar{q}$ and gluons G plus

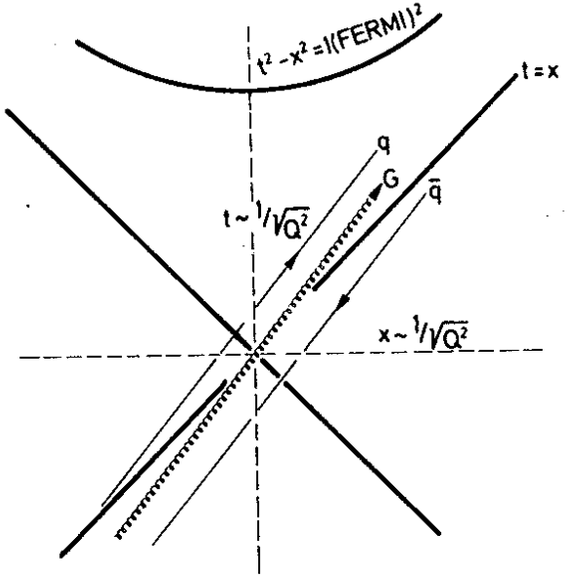

Fig.1

more $q\bar{q}$ pairs. These constituents come out of the distant past, and are travelling on or very near the light cone. At times and distances long after the blow caused by the lepton scattering off q or $\bar{q}$, the pion again becomes a hadronic system without resolved constituents. The typical scale for this to happen is the proper time τ, $\tau^2 = 1\ \text{Fermi}^2 = t^2 - x^2$ (measured in Fermi with c = 1). This is the hyperbola on Fig. 1. Increasing Q^2 leads to a very slow perturbative proliferation in the number of resolved constituents seen at a distance scale $1/\sqrt{Q^2}$ [3]. Lowest order in $\alpha_s(Q^2) = g_s(Q^2)/4\pi = 12\pi/(33 - 2N_F)\ln Q^2/\Lambda^2$ is the parton model. At some scale $Q_o^2 \sim$ 2-5 GeV^2 resolution into constituents first takes place. q, $\bar{q}$ and Gluons G become visible. (The gluons are visible only in principle, as they have no flavor and do not scatter leptons.) The gluons one sees at scale Q_o^2 are probably just the Lorentz-transformed potential. Positronium is a credible example. At rest one has e^+, e^- and a static Coulomb potential binding them. Boosted, the Coulomb field resembles a packet of nearly real photons (à la Weizsäcker and Williams) "confined" in a transverse area of dimensions $1/\alpha m_e$ and with wavelengths between $\sim 1/\alpha m_e$ and $1/P_z$ (the total lab momentum is P_z).

If the confinement potential is smooth, one can ignore it on a scale $1/\sqrt{Q^2} \ll$ Fermi. Its only effect is to provide the gluonic constituents of the target at this scale. Any remaining effects are survivors of the excited states of the system still visible at Q^2. Since the excitations of hadrons are all $\sim$ 1/2 GeV above the ground state, this is probably the scale of confinement effects - which are then negligible at large Q^2.

The space time picture of jet formation looks quite different[2]. A pair of constituents are made at t = o - in $e^+e^- \to q\bar{q}$, for example. The q and $\bar{q}$

pace apart at a small angle to the light cone t = x (Fig. 2).

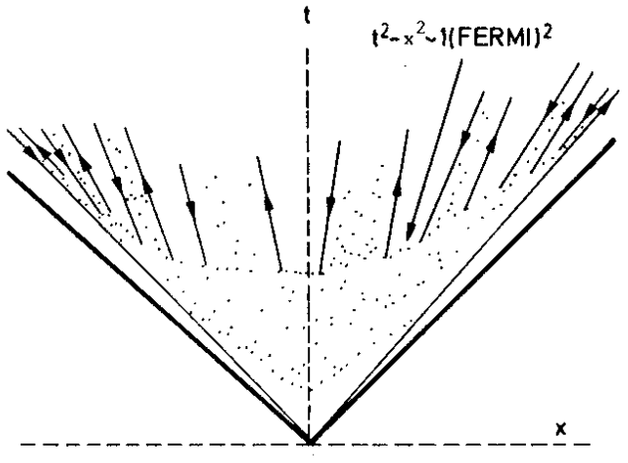

Fig. 2

If color is to be confined, the asymptotic states must be $q\bar{q}$, qqq and $\bar{q}\bar{q}\bar{q}$ states, including confined color fields in them with dimensions ~ Fermi. Moreover, there can be no strong color fields at times $O(1/\sqrt{Q^2})$, by asymptotic freedom. So the fields have to build up and then break up by $q\bar{q}$ creation. This is shown fancifully in Fig. 2. Since almost everything is relativistic, color compensation must be complete at proper times τ, $\tau^2 = t^2 - x^2 \sim 1(\text{FERMI})^2$. Otherwise color separates by large distances in a co-moving frame, and this is forbidden by our assumption that color is confined inside a scale ~ 1 Fermi. This is why essentially freely moving mesons emerge beyond the hyperbola $t^2 - x^2 \sim 1(\text{Fermi})^2$ in Fig. 2. Since color is compensated also over transverse distances at 1 Fermi (not shown) the particles come out in two jets, one along the q direction and the other along the $\bar{q}$

direction. This means p_T is of order $\langle p_T\rangle \sim 1/\text{Fermi}$ by the uncertainty principle.

Confinement effects are very different here, compared to deep inelastic scattering. Their scale is essentially given by the fluctuations in this long distance hadronization process. One simple estimate of their size is the following. Fig. 3 shows a rapidity plot of the two jets

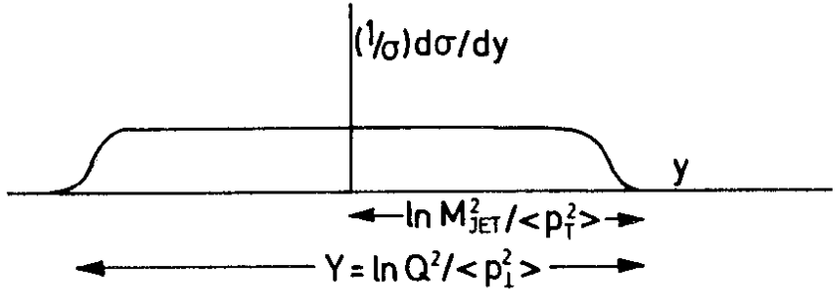

Fig. 3

The total rapidity range is just $Y_{TOT} = \ln Q^2/\langle p_T^2\rangle$ (ignoring hadron masses). The rapidity range of one jet is 1/2 Y_{TOT}. This is given by $\ln M^2_{JET}/\langle p_T^2\rangle$, where M_{JET} is the CM energy of the jet in its own rest frame (the invariant mass at all hadrons making up the jet). This is

$$\langle M^2_{JET}\rangle = \sqrt{Q^2\langle p_\perp^2\rangle} \sim .4\sqrt{Q^2}\ \text{GeV}^2 \qquad (1)$$

"Confinement" is only totally irrelevant when $\langle M^2_{JET}\rangle \ll Q^2$. Even at very high Q^2 it may become important for some values of the relevant kinematic variables.

2. Minimal Data Summary

The size of nonperturbative confinement effects can be judged from $e^+e^- \to$ 2 jet data at low energies (SPEAR and DORIS). Data is usually analyzed in terms of sphericity or thrust.[4]

Sphericity. Consider the 3 x 3 matrix

$$S^{\alpha\beta} = \sum_i \left(\delta^{\alpha\beta} \vec{p}_i^{\,2} - p_i^\alpha p_i^\beta \right) \qquad (2)$$

where $\alpha, \beta = 1,2,3$ (or x, y and z) and i labels the final state hadrons. This is easily diagonalized. This gives eigenvectors $\hat{e}_1, \hat{e}_2, \hat{e}_3$ and eigenvalues which can be ordered as $\lambda_3 \le \lambda_2 \le \lambda_1$. It is clear that $\sum (\vec{p}_{i\perp})^2 = \lambda_\alpha$, where $\vec{p}_{i\perp}$ is defined relative to the eigenvector $\hat{e}_\alpha$. λ_3 is then the absolute minimum $\lambda_3 = \text{MIN} \sum_i (\vec{p}_{i\perp})^2$ and the sphericity is just

$$S = \frac{3\lambda_3}{\lambda_1+\lambda_2+\lambda_3} = \frac{3}{2} \frac{\text{MIN} \sum_i (\vec{p}_{i\perp})^2}{\sum_i \vec{p}_i^{\,2}} \qquad (3)$$

The eigenvector $\hat{e}_3$ defines the best jet axis, and $\hat{e}_2$ and $\hat{e}_3$ define a plane of the event.

Thrust. This is defined by

$$T = \frac{\text{MAX} \sum_i |\vec{p}_i \cdot \widehat{\text{AXIS}}|}{\sum_i |\vec{p}_i|} \qquad (4)$$

and it finds the best axis such that the sum of absolute values of parallel momenta is maximized. Why use thrust? A simple calculation will make this clear. Take two partons of momenta P and P' as in Fig. 4.

Fig.4

Suppose that they fragment into n and n' hadrons each parallel to its parent and with momentum P /n, P' /n'. The sphericity and thrust of the partons (hadrons) are

$$S_{\text{PARTON}} = \frac{3}{2} \text{MIN} \frac{P^2 \sin^2\delta + P'^2 \sin^2\delta'}{P^2 + P'^2} \quad \neq \quad S_{\text{HAD}} = \frac{3}{2} \text{MIN} \frac{P^2 \sin^2\delta/n + P'^2 \sin^2\delta'/n'}{P^2/n + P'^2/n'} \qquad (5)$$

$$T_{\text{PARTON}} = \text{MAX} \frac{P\cos\delta + P'\cos\delta'}{P + P'} = T_{\text{HAD}} = \text{MAX} \frac{P\cos\delta + P'\cos\delta'}{P + P'}$$

In the limit where all (or almost all) hadrons are parallel to a parton, the thrust of the partons and hadrons are the same. This is because thrust

is linear in momenta. Sphericity does not have this nice feature.[4]

It is well known that at SPEAR energies one can find a jet axis.[5] The parton level reaction is $e^+e^- \to q\bar{q}$. In the limit of zero quark mass, the cross section has an angular dependence $1 + \cos^2\theta$. (θ is the angle of the jet axis to the beam direction). This follows by a helicity argument (Fig. 5).

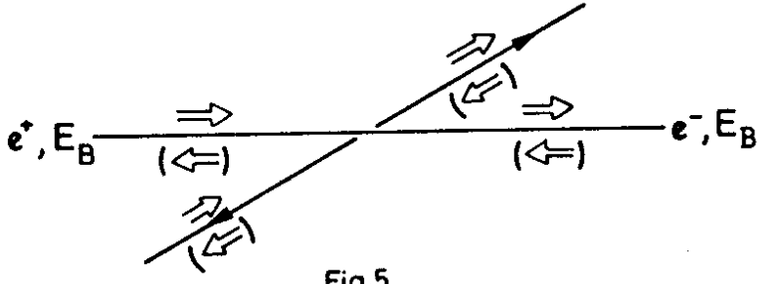

Fig.5

Massless e^+e^- only annihilate in a state where the spins are parallel or for $J_z = \pm 1$. The same is true for the final state. The angular factor for a state of $J_z = \pm 1$ (z along P_e) to go to a state with $J_{z'} = \pm 1$ (z' along P_q) is $1 + \cos^2\theta$ (see your particle data group booklet). The exact cross section for zero $e^\pm$ mass and fermion mass M_F is

$$\frac{d\sigma}{d\cos\theta} = \sum e_i^2 \frac{\pi\alpha^2}{8E_B^2}\left(1 - \frac{M_F^2}{E_B^2}\right)\left[1 + \cos^2\theta + \frac{M_F^2}{E_B^2}(1 - \cos^2\theta)\right] \qquad (6)$$

The coefficient of $1 + \cos^2\theta$ is usually called σ_T and that of $1 - \cos^2\theta$ is σ_L. From SPEAR jet data at $2E_B = 7.4$ GeV, $\sigma_L/\sigma_T = .02 \pm .07 < .09$ (1σ level). So the outgoing particles are fermions. But using this to get

a bound on M_F^2 from (6), $M_F < .09\ E_B = 1.1$ GeV - not a very significant limit. This cannot really distinguish between M_q in (6) or, say, $\langle M_{JET} \rangle$ ($\langle M_{JET} \rangle \approx 1.7$ GeV at 7.4 GeV).

The actual evidence for two jet events is shown in Fig. 6.[5] This compares the p_T and $x = 2p/E_B$ distributions (p_T defined relative to the jet axis) at one energy (7.4 GeV). Notice that there is a significant difference between the data and a phase space model. The model has no correlation with a jet axis. It simply distributes the observed number of particles in phase space, taking account of energy and momentum conservation. Equally interesting is the fact that the jet and phase space models are numerically not so very different. Once having found a jet axis in a random event, the p_T's are automatically made smaller than the longitudinal momenta. (Of course, no phase space model could reproduce the $1 + \cos^2\theta$ distribution of the axis.)

Clearly, jets at low energy are not very narrow. This is even clearer from PLUTO data at DORIS, $2E_B = 9.4$ GeV. They plot the average fraction of the total energy outside a cone of half opening angle δ (Fig. 7).[6] Even at this energy, a cone containing an average 60 % of the energy has a solid angle of ≈ 1 steradian. This mean opening angle ought naively to scale as $1/E_B$. So a typical 15 GeV jet at PETRA would occupy a solid angle of about 0.1 steradians. This is much better. It is this shrinkage of jet opening angles which makes a search for multijet events feasible at $2E_B \approx 30$ GeV.

Another way to gauge the size of nonperturbative jet opening angles is through the mean sphericity or thrust. Naively,

$$\langle S \rangle_{2\,JET} \sim \frac{3}{2}\frac{\langle p_\perp^2 \rangle}{\langle p^2 \rangle} \sim \langle N_{HAD} \rangle \frac{\langle p_\perp^2 \rangle}{Q^2} \qquad (7)$$

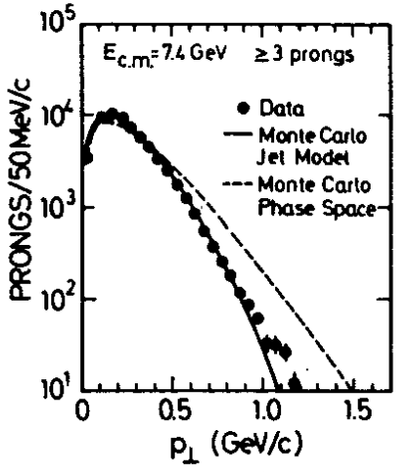
$E_{c.m.}$=7.4 GeV ≥3 prongs
Data
Monte Carlo Jet Model
Monte Carlo Phase Space
PRONGS/50MeV/c
$p_\perp$ (GeV/c)

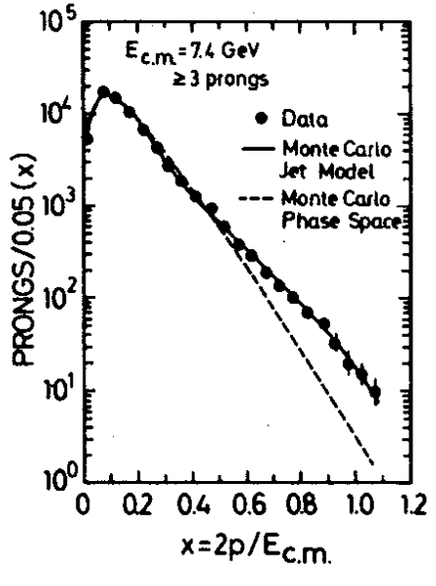
$E_{c.m.}$=7.4 GeV
≥3 prongs
Data
Monte Carlo Jet Model
Monte Carlo Phase Space
PRONGS/0.05 (x)
x=2p/$E_{c.m.}$

Fig. 6

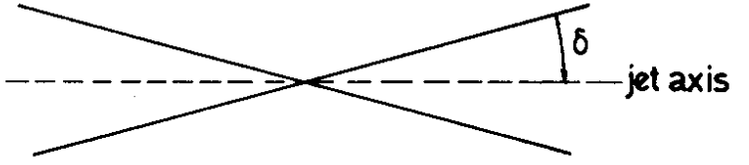
δ
jet axis

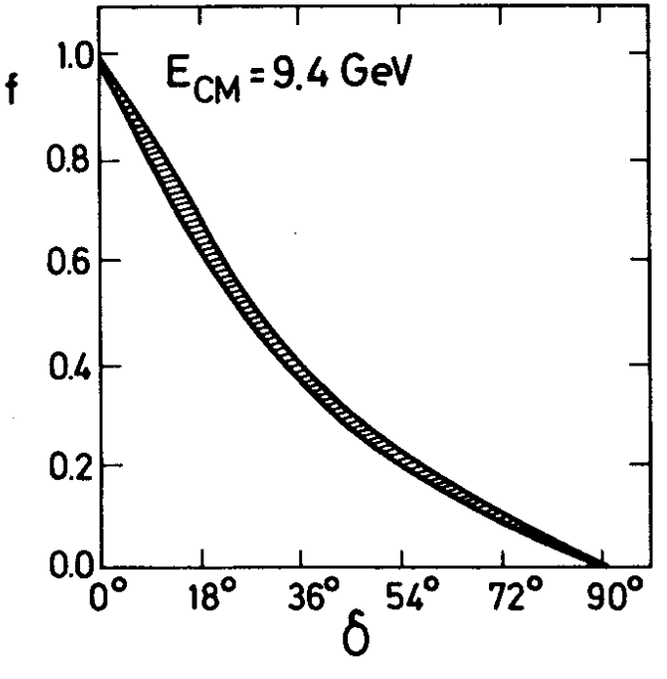
E_{CM} = 9.4 GeV
f
δ

Fig. 7

This is tiny at PETRA energies. It is also wrong. The reason is clear from Fig. 6. There are many particles of low momentum. They lower $\langle p^2 \rangle$ and increase $\langle S \rangle$ compared to (7). An empirical fit to $2E_B \lesssim 10$ GeV data gives

$$\langle S \rangle_{2JET} \sim .55\, E_B^{-.5} \tag{8}$$

The smearing effects of confinement will clearly be important all through the PETRA energy range. But they are small enough at 30 GeV to be easily controlled, as we will see.

Notice again that confinement effects are quite different here, compared to deep inelastic reactions. A typical non-singlet moment of a structure function is[1,7]

$$M^{NS}(n, Q^2) = A_n \left[\frac{\ln Q^2/\Lambda^2}{\ln Q_0^2/\Lambda^2} \right]^{-d_n} + \sum C_k \left(\frac{\mu_n^2}{Q^2} \right)^k \tag{9}$$

Since the only mass scales are M_p or Λ (both of order GeV), the last ("higher twist") term in (9) is negligible for $Q^2 \gg M_p^2$, Λ^2 provided the sum makes sense. The advantage in e^+e^- reactions is, of course, that $Q^2 \sim 1000$ GeV^2 compared to $Q^2 \sim 100$ GeV^2 in ℓN.

II. Perturbative QCD Tests

Jets at PETRA and PEP energies will be narrow, so we can exploit this in tests of QCD. We look for the distributions of jets from QCD quanta produced at short distances. The interesting processes involve hard noncollinear radiation. Then short distances dominate. Fig. 8 shows these processes in analogy to QED. Both theories contain fermions coupled to massless vector quanta. At short distances the QCD coupling is not large. The characteristic expansion parameter at PETRA/PEP energies is $\alpha_s/\pi \sim .07$. Since this is fairly small, we will be interested only in low orders of perturbation theory. Then the color of the gluon plays little role (with an exception we mention later). These processes are an ideal tool to establish the existence and properties of the gluon.[4]

Yet another comparison with deep inelastic scattering may be useful. There one looks for violations of Bjorken scaling.[7] These arise from gluon emission before the lepton scatters on a q or $\bar{q}$ at distance scale $\sim 1/\sqrt{Q^2}$ This radiation is mostly collinear. It degrades the longitudinal momentum of the q or $\bar{q}$ (Fig. 9).[3]

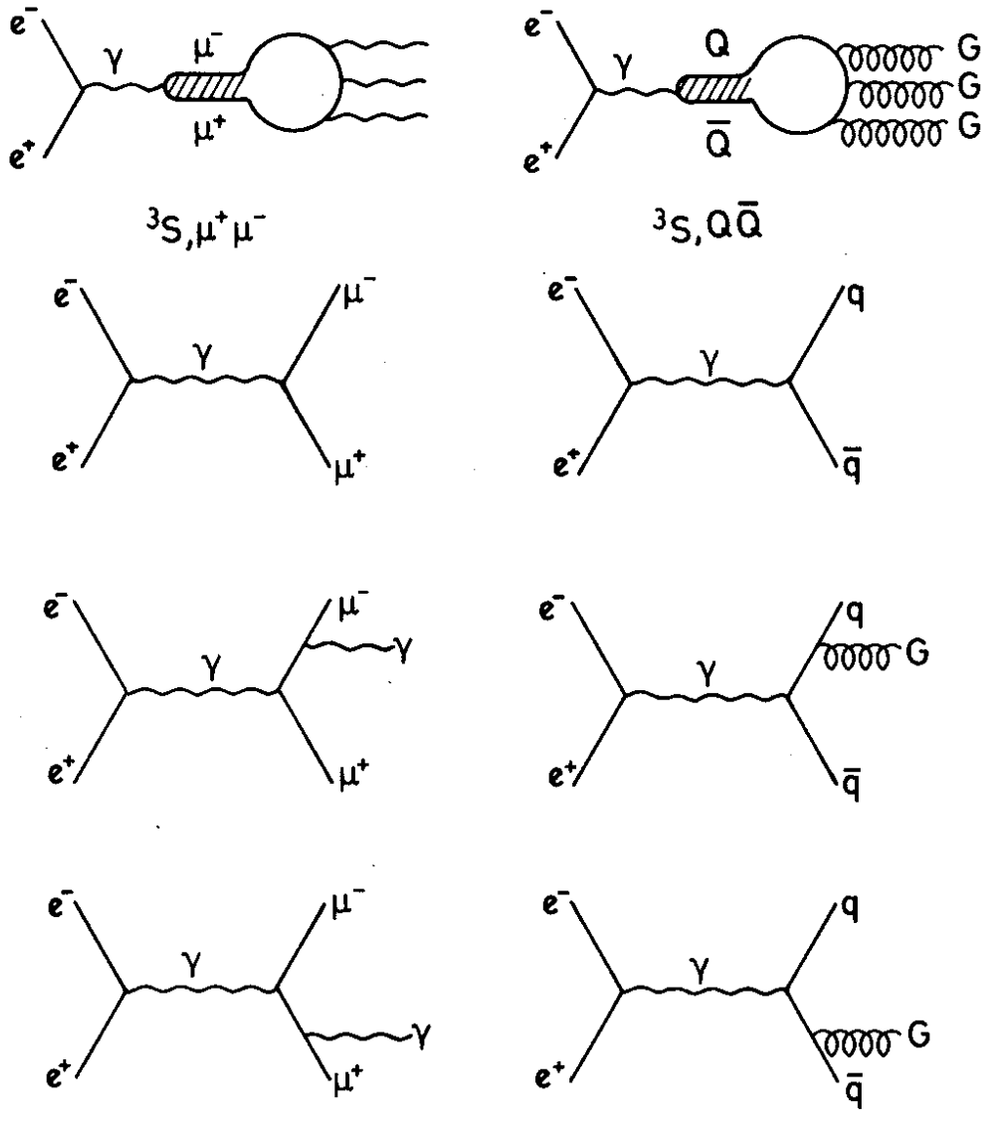

Fig.8

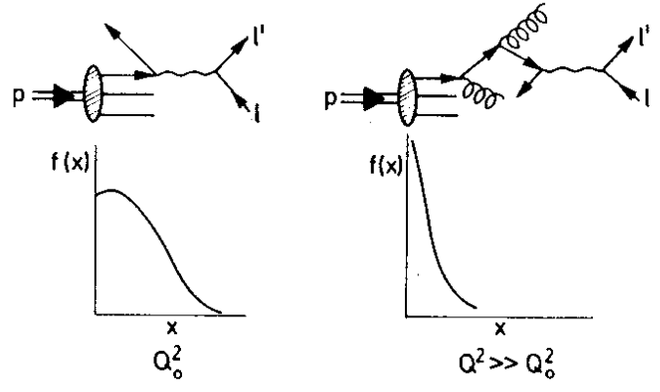

Fig.9

By contrast, we will look at noncollinear processes.

Three Body Kinematics

The processes in Fig. 8 all involve three massless or nearly massless quanta. The kinematics are fixed by scaled parton momenta $x_i = |\vec{p}_i| / E_B$, where $x_1 + x_2 + x_3 = 2$, and by the angles between any two partons i and j,

$$\cos\theta_{ij} = 1 - \frac{2(1-x_k)}{x_i x_j} \qquad (10)$$

where k is the third. (See Fig. 10). The three x_i can be put on a Dalitz plot (Fig. 11) Along the edges two quanta are parallel, and at the center they are equally energetic and 120° apart in angle. This three-quantum state has thrust $T = \mathrm{MAX}(x_1, x_2, x_3)$ and the Dalitz plot splits into 3 sectors, depending on whether 1, 2 or 3 defines the T axis. The differential rate is proportional to $|\mathcal{M}|^2 \, dx_1 dx_2$. Ideally one would like to plot jet cross sections this

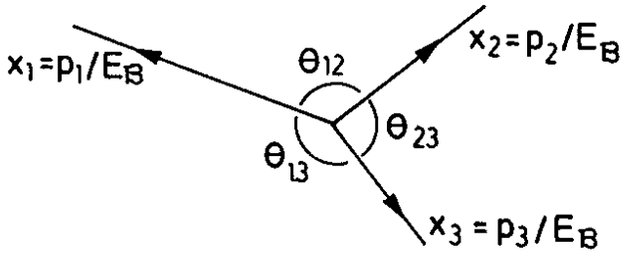

Fig.10

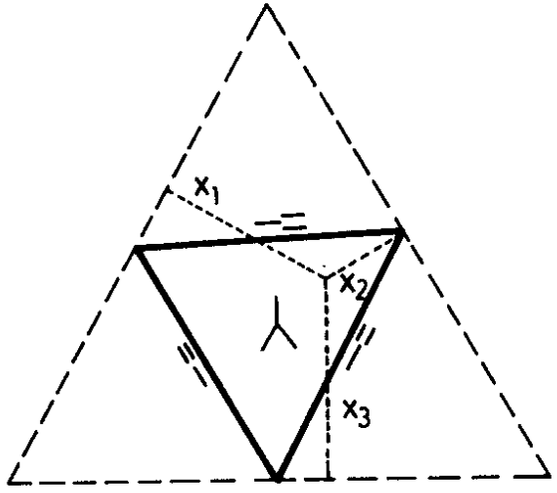

Fig.11

way (a jet Dalitz plot).

There are two convenient ways to describe the spatial orientation of this system. One is via the normal to the plane of the three quanta,

and the other is via the orientation of the thrust axis (the direction of the most energetic quantum). This is shown on Fig. 12.

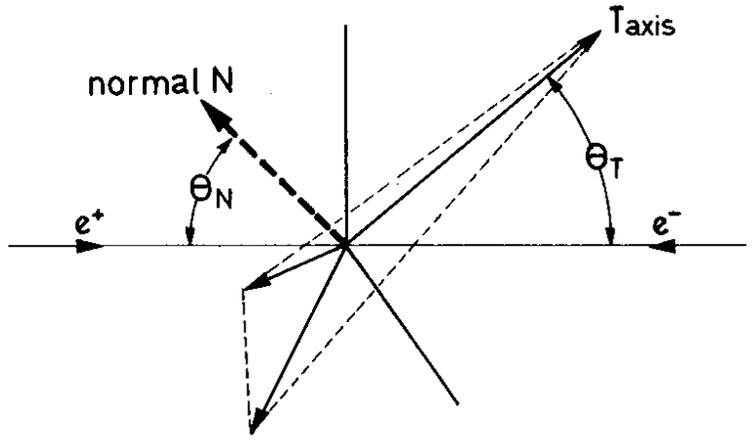

Fig.12

These distributions for an initial virtual photon must be

$$\frac{d\sigma}{d\cos\theta_N} \propto 1 + \alpha_N \cos^2\theta_N$$

and (11)

$$\frac{d\sigma}{d\cos\theta_T} \propto 1 + \alpha(T) \cos^2\theta_T$$

Although (11) are not the complete angular distributions, they contain all the physics we need. (Notice that α_N is independent of x_1, x_2, x_3 but $\alpha(T)$ is not.) From now on, we assume that azimuthal angles not designated on Fig. 12 have been averaged over.

A. $Q\bar{Q} \rightarrow GGG \rightarrow$ 3 JETS

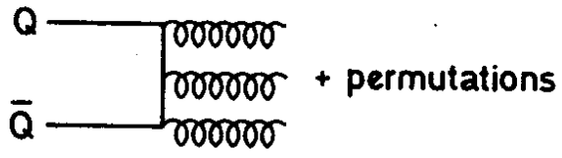

Fig.13

Fig. 13 shows the Feynman diagrams for the decay of a heavy $J^{PC} = 1^{--}$ $Q\bar{Q}$ pair[8] to three gluons. The fractional decay rate is[9]

$$\frac{1}{\Gamma}\frac{d\Gamma}{dx_1 dx_2} = \frac{3}{2(\pi^2-9)}\left[\frac{(1-x_1)^2}{x_2^2 x_3^2} + \frac{(1-x_2)^2}{x_1^2 x_3^2} + \frac{(1-x_3)^2}{x_2^2 x_1^2}\right] \qquad (12)$$

Despite its appearance, (12) is finite for any $x_i \rightarrow 0$. A three dimensional plot of (12) versus x_1, x_2, x_3 on the Dalitz triangle is shown on Fig. 14.[10]

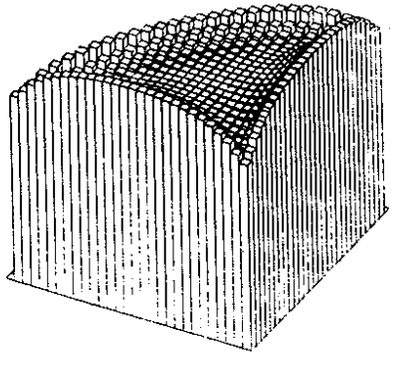

Fig. 14

It is remarkably uniform.

Before (12) can be used to test QCD we need to know what fraction of the total $Q\bar{Q}$ decay rate is to 3G. Two other modes are $Q\bar{Q} \rightarrow 1\gamma \rightarrow e^+e^- + \mu^+\mu^- + \tau^+\tau^- + q\bar{q}$ and $Q\bar{Q} \rightarrow \gamma 2G$.[8] Asymptotically, the ratio $\Gamma(Q\bar{Q} \rightarrow GGG)/\Gamma(Q\bar{Q} \rightarrow \text{all})$ can be calculated from lowest order QCD and $\alpha_s(Q^2 = M^2_{Q\bar{Q}})$. This is shown on Fig. 15. Unfortunately,

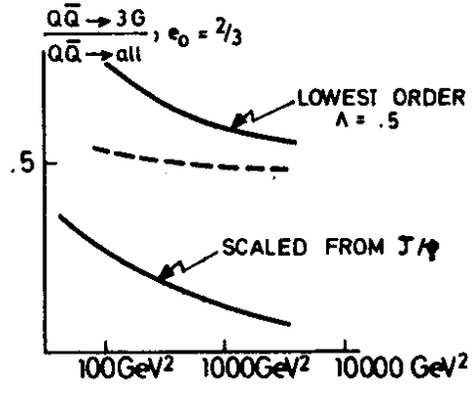

Fig. 15

this calculation fails by a factor of order 6-8 for J/ψ. On Fig. 15 we show the J/ψ value, scaled as $(\ln M^2/\Lambda^2)^{-3}$ at higher M^2. (In both cases, $\Lambda = .5$ GeV). If the lowest order calculation is in fact correct at large M^2, the actual value must somehow interpolate between the J/ψ result and the asymptotic one. (An imaginary interpolation is shown on Fig. 15.) It is extremely important to know the total $\Upsilon(9.46) \rightarrow GGG \rightarrow$ Hadrons width. Scaling from J/ψ would indicate a direct width near 10 keV. The interpolation (if correct) would imply a width nearer 50 keV, and also a large branching ratio of the next

$Q\bar{Q}$ resonance to GG. Since this value is nearer the lowest order QCD value (around 100 keV), one would also worry less about whether or not the discrepancy of measured and calculated rates might also affect the 3 jet distributions (and thus the projected QCD test in $Q\bar{Q} \rightarrow$ 3jets).[11] Right now, $\Gamma(\Upsilon)$ is too poorly known to draw any conclusion.

From now on we assume that $\Gamma(Q\bar{Q} \rightarrow GGG)/\Gamma(Q\bar{Q} \rightarrow All)$ is large enough so that the three jet final state can easily be separated from

$$Q\bar{Q} \rightarrow 1\gamma \rightarrow q\bar{q} \rightarrow 2 \text{ jets}$$

and

$$Q\bar{Q} \rightarrow 1\gamma \rightarrow q\bar{q}G \rightarrow 3 \text{ jets}$$

(which is small - of order $\alpha_s/\pi \sim 7$ % of the $q\bar{q} \rightarrow$ 2 jet rate).

Angular Distribution of the Normal

This turns out to give us a nice test of the gluon spin in $Q\bar{Q}$ decay. For $Q\bar{Q} \rightarrow$ GGG with vector gluons, $\alpha_N = -1/3$ in equ. (11). For three scalar or pseudoscalar "gluons", the matrix element of the vector electromagnetic current is fixed by parity to be

$$\langle 3 \text{ scalar} | \vec{J}_{EM} | 0 \rangle \propto \text{linear combination of } \vec{P}_1, \vec{P}_2, \vec{P}_3$$

$$\langle 3 \text{ pseudoscalar} | \vec{J}_{EM} | 0 \rangle \propto \vec{P}_1 \times \vec{P}_2 \qquad (13)$$

Thus $\vec{J}_{em}$ points along the normal in the pseudoscalar case, and lies in

the 3 quantum plane for scalars. (It may, of course, have a vanishing coefficient.) Thus from spin considerations, $\alpha_N = -1$ for $J^P = 0^-$ gluons, and $\alpha_N = +1$ for scalars (table).[10] Agreement of data with $\alpha_N = -1/3$ would be a nontrivial success for QCD.

"GLUON" J^P	α_N
0^-	-1
0^+	+1
1^-	-1/3

Table

Angular distribution of the thrust axis

This also checks the gluon spin, as we can see from Fig. 16 in the limit

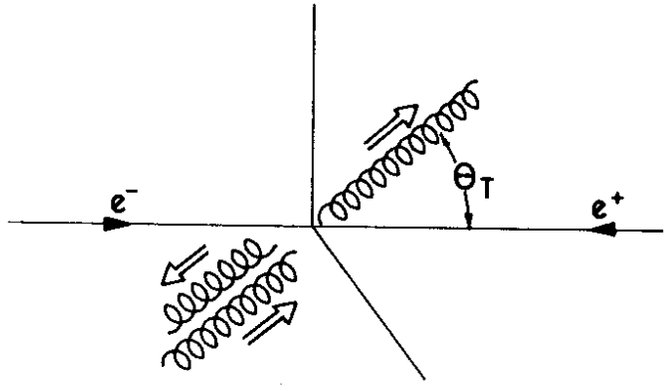

Fig.16

$T \rightarrow 1$ (the edges of the Dalitz plot, where gluon momenta are collinear).

Massless vector gluons can only have a spin projection ± 1 along the thrust axis. Thus from spin we get the $e^+e^- \to q\bar{q}$ result[10]

$$\lim_{T\to 1} \alpha(T) = +1$$

whereas scalar gluons have spin projection o along the thrust axis and the collinear case has

$$\lim_{T\to 1} \alpha(T) = -1$$

(as for $e^+e^- \to \pi^+\pi^-$). Koller and Krasemann have worked out the scalar case more carefully and find the <u>average</u> $\langle \alpha_{SCALAR}(T) \rangle \approx -1$ (averaged over all T).[12] The thrust distribution from (12) is shown together with $\alpha_{QCD}(T)$ [13] and $\alpha_{SCALAR}(T)$ in Fig. 17. PLUTO data[14] for Y(9.46) as shown on Fig. 18, compared to

"$Q\bar{Q} \to$ 2 JETS"

and

"$Q\bar{Q} \to$ no JETS" (phase space)

The $Q\bar{Q} \to$ 3 jet model employs a Monte Carlo treatment of $G \to$ hadrons fragmentation. What we have been calling the nonperturbative jet broadening, is clearly important. But the data also agrees with the 3 jet model and not the others. Also, note that the evidence for planarity in the plot of P_{out} (p_{out} is perpendicular to the event plane) is about as significant as the

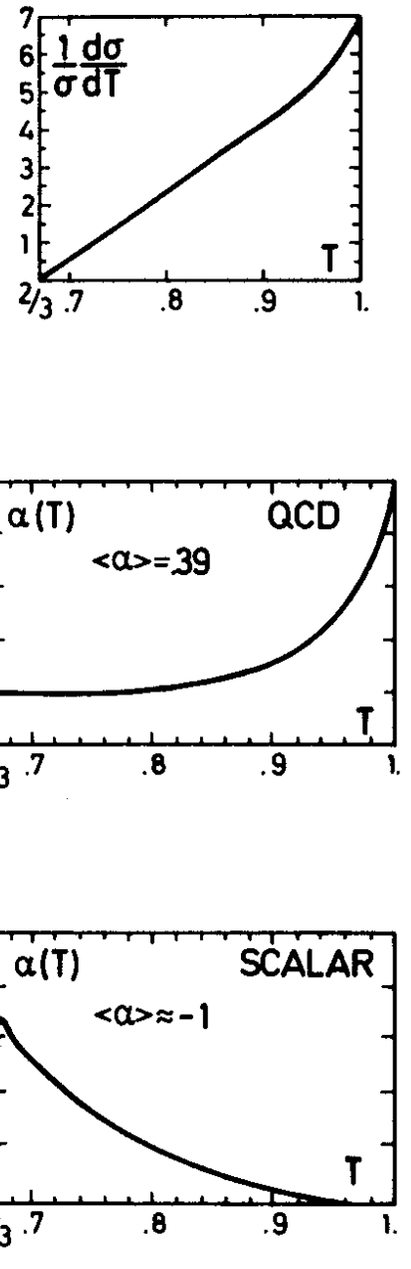

Fig. 17

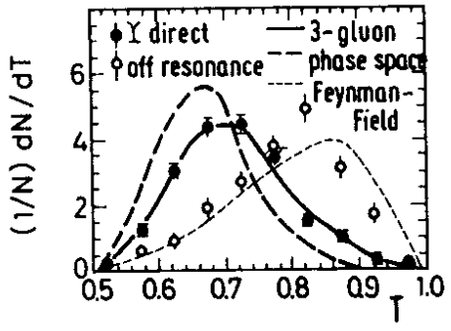

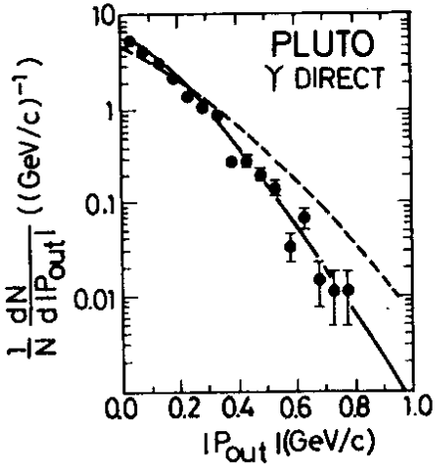

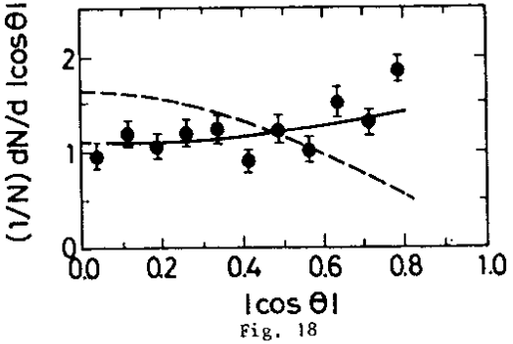

Fig. 18

evidence for limited p_T in $e^+e^- \rightarrow$ 2 jets at SPEAR (Fig. 6). This is important, as it is independent of the thrust distribution. Finally, the angular distribution of the thrust axis is compared to QCD (solid line) and the scalar model (dashed line).

Clearly it would be better to have a heavier $Q\bar{Q}$ resonance. But the agreement with QCD is pretty striking.

It's amusing to speculate what would happen to this agreement if the gluon dominating short distance processes had no color. Then the leading process is that in Fig. 19 (for a vector gluon with no color). The decay is then

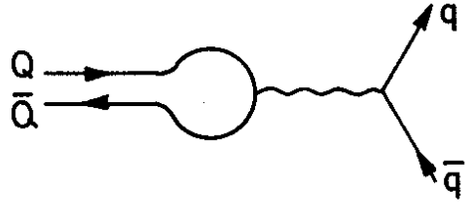

Fig.19

$Q\bar{Q} \rightarrow G \rightarrow q\bar{q} \rightarrow$ 2 jets. This is excluded. So here, too, the agreement with QCD's colored gluons is nontrivial.[15]

Gluon Flavor

If the predicted $Q\bar{Q} \rightarrow$ GGG mechanism is correct, the final state should show evidence of the gluons' lack of flavor.[13] We simply look at an energetic particle (e.g. a $\pi^{\pm}$) in low sphericity events. $Q\bar{Q} \rightarrow$ GGG decay implies that the particles on the other side know nothing of this flavor selection. Off the

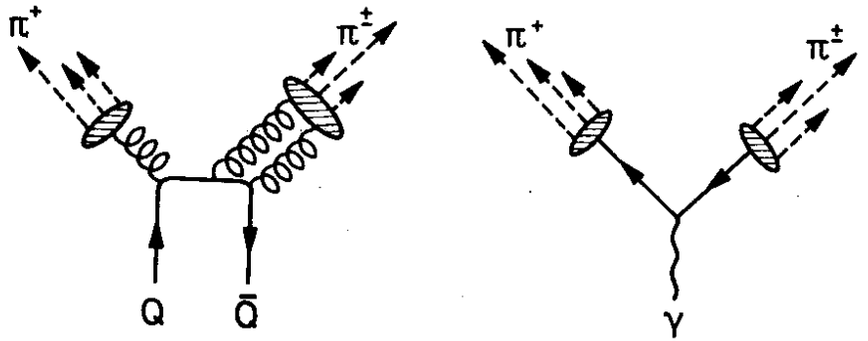

Fig.20

resonance, for $e^+e^- \to q\bar{q}$, selecting an energetic $\pi^\pm$ in one jet biases us to find $\pi^\mp$ in the other. Defining a correlation between opposite jets,

$$C(\pi^+,\pi^\pm) = \int_{z_0}^{1} dz_1 \int_{z_0}^{1} dz_2 \, \frac{1}{\sigma} \frac{d\sigma(\pi^+,\pi^\pm)}{dz_1 dz_2} \qquad (14)$$

($z_0 = p_\pi^{min}/E_B$) we show C for e^+e^- and Υ decays in Fig. 21.[13] There is not yet sufficient Υ data to carry out this check.

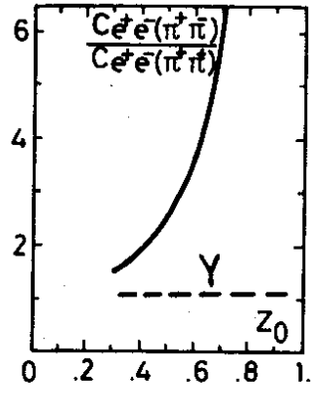

Fig. 21

B. $e^+e^- \to q\bar{q} + q\bar{q}G \to$ 2 jets + 3 jets

There are many diagrams through order $g_s^2(Q^2)$ in amplitude (Fig. 22). We are only interested in the two and three jet processes at the top of the page.[16] The loop correction to $e^+e^- \to q\bar{q}$ is trivially included by probability conservation. The total cross section is

$$\sigma(e^+e^- \to HAD) = 3\sum e_i^2 \sigma_{\mu^+\mu^-}\left(1 + \frac{\alpha_s(Q^2)}{\pi} + C\left(\frac{\alpha_s(Q^2)}{\pi}\right)^2 + \dots\right) \qquad (15)$$

Up to this order the three jet rate can be easily calculated. The two jet rate is just σ(3 jet) - σ(total). One might worry that the next order corrections to $q\bar{q}G$ will be large. (They have not yet been calculated.) This is unlikely, since $e^+e^- \to q\bar{q}q\bar{q}$ and $e^+e^- \to q\bar{q}GG$ have been calculated,[17] and so has C in equ. (15).[18] The first is small, and so is the second in an appropriate subtraction scheme.[18] From now on we assume that corrections to $q\bar{q}$ + $q\bar{q}G$ are small at PETRA/PEP energies, so long as one stays away from the kinematic region where long distances dominate anyway. (This is the collinear region near the edges of the $q\bar{q}G$ Dalitz plot.)

We can now find many quantitative predictions which depend only very weakly on the details of q, G jet formation.[19] The idea is the following (Fig. 23). Two jet events are those originating from $e^+e^- \to q\bar{q}$ (thrust T = 1). Three jet events originate from $e^+e^- \to q\bar{q}G$ at thrust $T < 1$. The invariant mass of the partons opposite that which determines T is $p^2 = Q^2(1-T)$. For $p^2 \ll Q^2$, this can be identified with the invariant mass of a q or $\bar{q}$ which subsequently

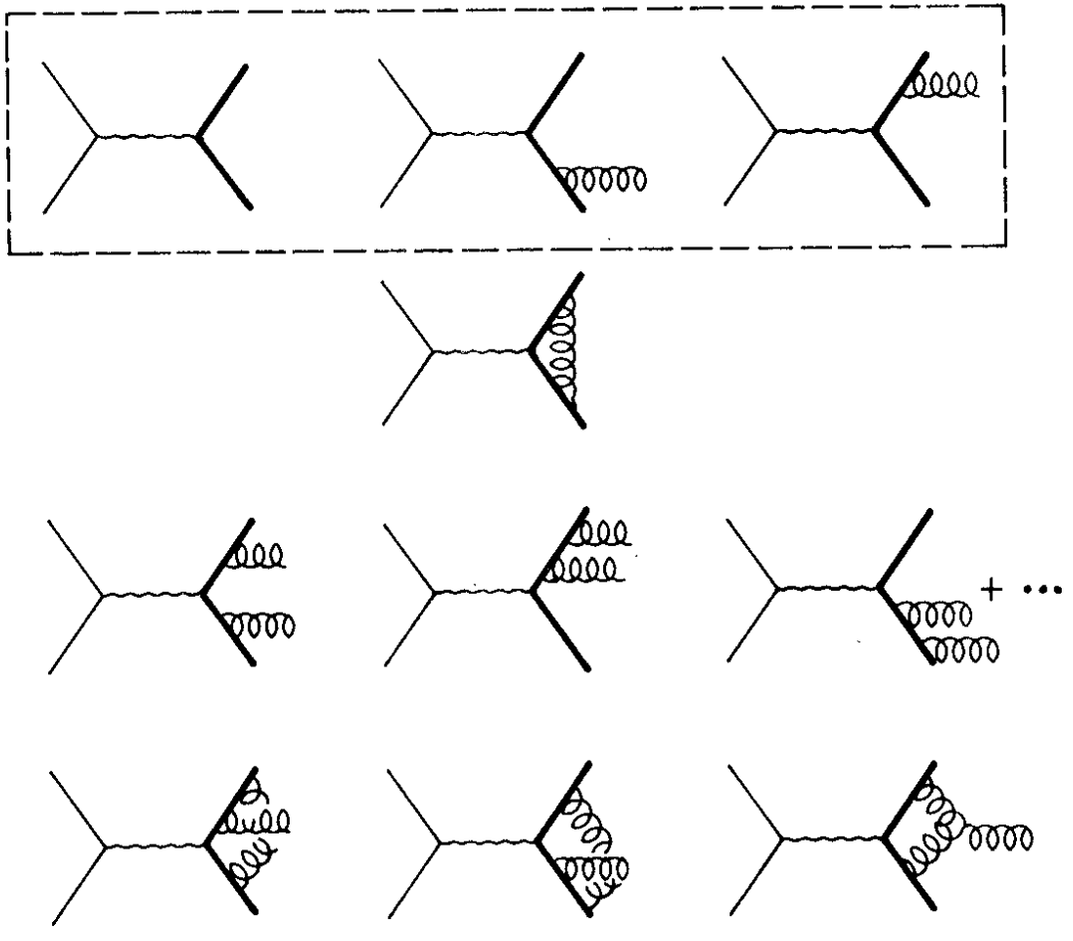

Fig. 22

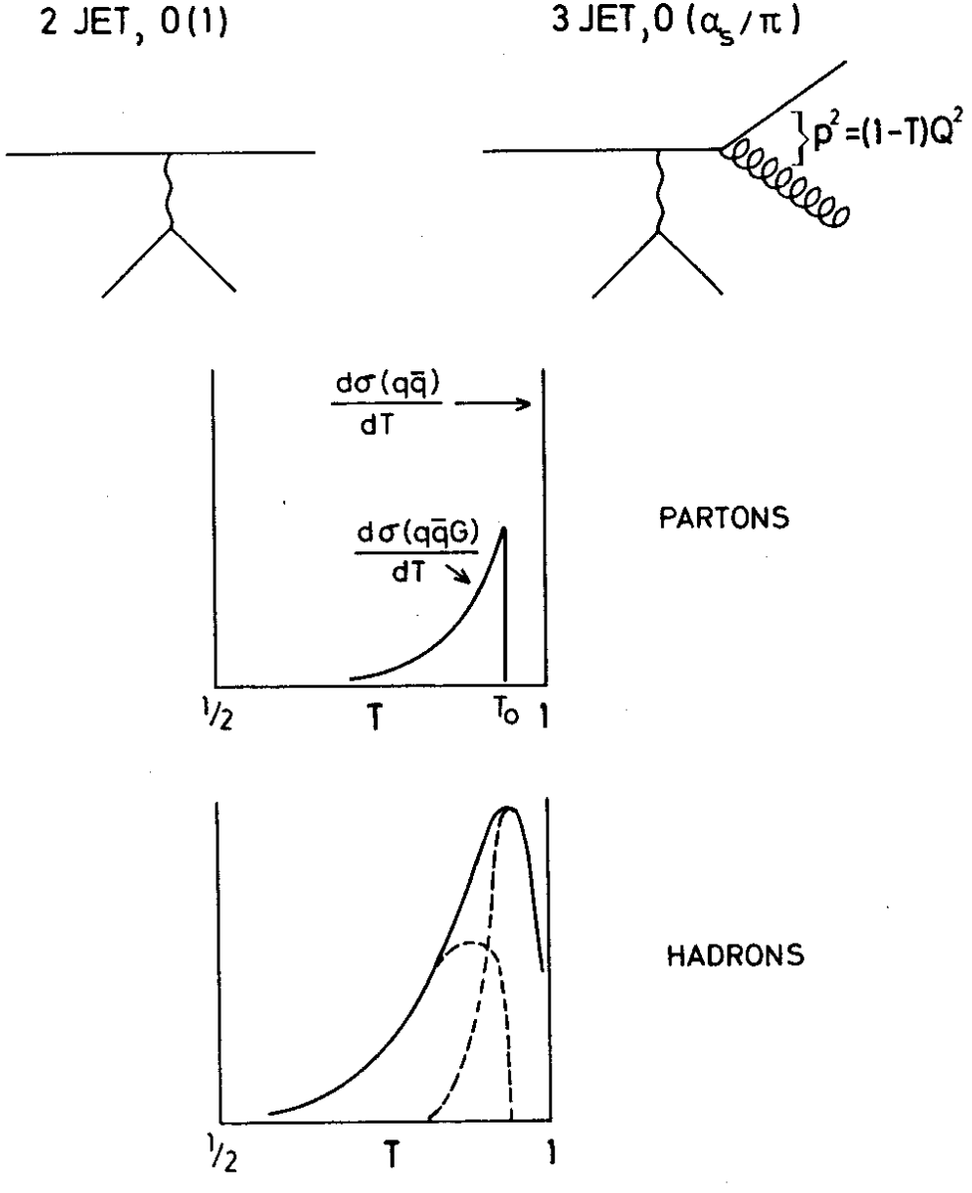
2 JET, O(1)
3 JET, O (αs/π)
p²=(1-T)Q²
dσ(qq̄)/dT
dσ(qq̄G)/dT
PARTONS
HADRONS
1/2
T
To
1
1/2
T
1

Fig. 23

radiates a gluon G. The $q\bar{q}G$ density on the Dalitz plot is[16] (Fig. 24 for x_q and $x_{\bar{q}}$ ≤ .8)

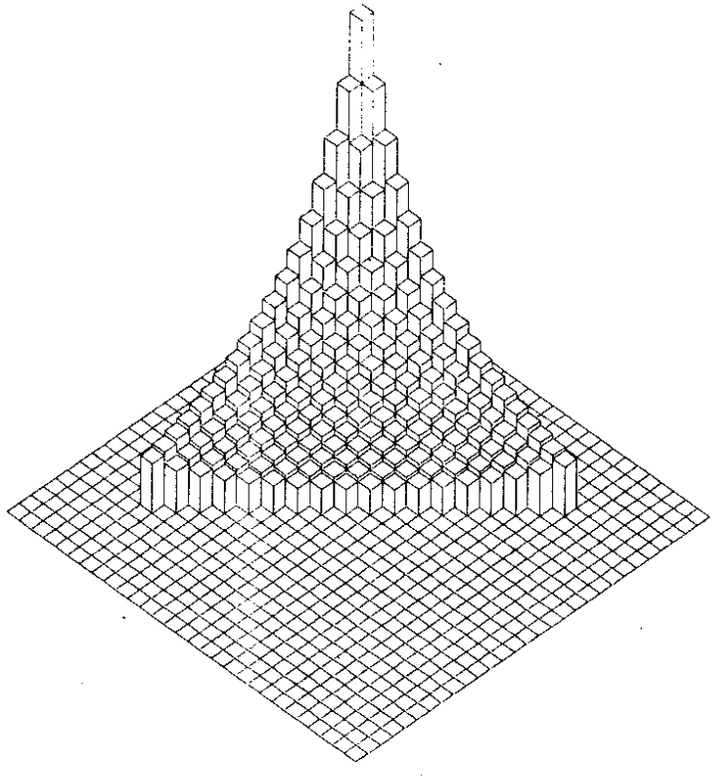

Fig. 24

$$\frac{1}{\sigma_0}\frac{d\sigma}{dx_q\,dx_{\bar{q}}} = \frac{2}{3}\frac{\alpha_s}{\pi}\frac{x_q^2 + x_{\bar{q}}^2}{(1-x_q)(1-x_{\bar{q}})} \tag{16}$$

It diverges for $T \to 1$, just as does $e^+e^- \to \mu^+\mu^-\gamma$. To define a reasonable (perturbatively small) $q\bar{q}G$ cross section we have to cut (16) off at some $T = T_0$. This is done with a sharp cut at thrust T_0. T_0 is chosen empirically to get a smooth hadronic thrust distribution after q, $\bar{q}$ and G fragmentation (Fig. 23). Since this cutoff is on the boundary where long distance effects play a role, we have to make sure that nothing depends strongly on it, just as we have to make sure that nothing we calculate depends strongly on quark or gluon fragmentation.

A comment about this cutoff is in order. Suppose that we calculate the laboratory range of the virtual parton of mass $P^2 = Q^2(1-T)$. Its lifetime against $q \to qG$ decay in its rest frame is $O(1/\sqrt{P^2})$. Lorentz dilated in the lab, this gives a travel distance before decay

$$\tau\gamma \sim \frac{1}{\sqrt{P^2}}\frac{E_B}{\sqrt{P^2}} = \frac{E_B}{P^2} \tag{17}$$

If this distance is large - of order $1/\Lambda$, where $\Lambda \sim 1/2$ GeV is the intrinsic scale parameter of QCD - then confinement effects must play a role. This is because the strong confining potential acts when we try to separate colored partons by such large distances. The p^2 at which we may have to worry about confinement is thus of order

$$\sqrt{p_c^2} = \sqrt{E_B\Lambda} \tag{18}$$

This is compared to our empirical cutoff in the following table, The empirical T_o was simply that thrust value where $e^+e^- \rightarrow q\bar{q} \rightarrow$ two jets reaches its maximum, as determined by the model of Field and Feynman.

Q^2	T_o	$\sqrt{(1-T_o)Q^2}$	$\sqrt{E_B \Lambda}$
15 GeV	.92	4.2 GeV	2.0 GeV
30 GeV	.95	6.7 GeV	2.7 GeV
90 GeV	.98	12.7 GeV	4.7 GeV

From these figures it ought to be clear that the merging of the 3 jets with the two jet configuration is not solely a perturbative question. This is one more reason to avoid calculating anything with a marked dependence on T_o.[20] (It is also clear that at energies much above 30 GeV we will have to include the possibility that $e^+e^- \rightarrow q\bar{q}GG \rightarrow$ 4 jets.)

What should we choose for $\alpha_s(Q^2)$? We took $\alpha_s = .20$, corresponding to five flavors, $Q^2 = 4E_B^2 = 1000$ GeV^2, and $\Lambda = .50$ GeV. Changing the number of flavors, Λ and also Q^2 to $Q^2(1-T_{min}) = Q^2/3$ indicates that there is at least a $\pm$ 10 % uncertainty in the proper value of α_s.[21] This is about what one would expect, since corrections from the next order diagrams ought to be $\sim \frac{\alpha_s}{\pi} \sim 10\%$

It is not too instructive to go through the calculations in detail. They can be found in ref. (19). Our aim was to get quantitative predictions before data became available. So we did everything we could in two different ways.

1. Analytically

We take $e^+e^- \rightarrow q\bar{q} + q\bar{q}G$ and assume that the fragmentation of q, $\bar{q}$ or G can be represented as

$$\frac{dN_{HAD}}{dz\, d p_\perp^2} \propto \frac{(1-z)^n}{z} e^{-p_\perp^2/\langle p_\perp^2 \rangle} \qquad (19)$$

(Actually, one plot - the total average $\langle p_\perp^2 \rangle$ over all hadrons relative to the T axis - was calculated in a way less dependent on fragmentation than (19) is.) We varied the $z = P_{HADRON}/E_{PARTON}$ distributions for q and G jets, to check the sensitivity to them. It is very weak. We also varied T_o. Above about $\sqrt{Q^2} \approx 20$ GeV this dependence is small for the quantities which will be shown. It turns out that within $\pm$ 10 - 20 % one can analytically and reliably calculate more things than one might think. We need no Monte Carlo. However,

2. Monte Carlo

we also develop a Monte Carlo model of $e^+e^- \rightarrow q\bar{q} + q\bar{q}G$. In the range $2/3 \leq T \leq T_o$, $q\bar{q}G$ momenta are chosen according to (16). The rate for $e^+e^- \rightarrow q\bar{q}$ is given by

$$\sigma(q\bar{q}) = \sigma_{TOT} - \int_{2/3}^{T_o} \frac{d\sigma(q\bar{q}G)}{dT}\, dT \qquad (20)$$

q and $\bar{q}$ fragment as in the standard q = u,d,s Field and Feynman model.[22] (We need not include c, b as we already know that this would be a 10 % refinement, from our analytic calculations.) Finally, a G jet is just like a q or $\bar{q}$ jet except that the quantum numbers are fixed to be neutral by treating it as a coherent $q\bar{q}$ pair. (The q or $\bar{q}$ are only kept to ensure that the different meson flavors are averaged over in a random way.) Such Monte Carlo programs are useful for experimentalists. This said, Fig. (25) shows the global $\langle p_T^2 \rangle$ relative to the thrust axis, averaged over all events. The solid curve is from the Monte Carlo. The dashed curve is the analytic result, normalized to the Monte Carlo value below E_{cm} = 10 GeV. The agreement is very satisfying.

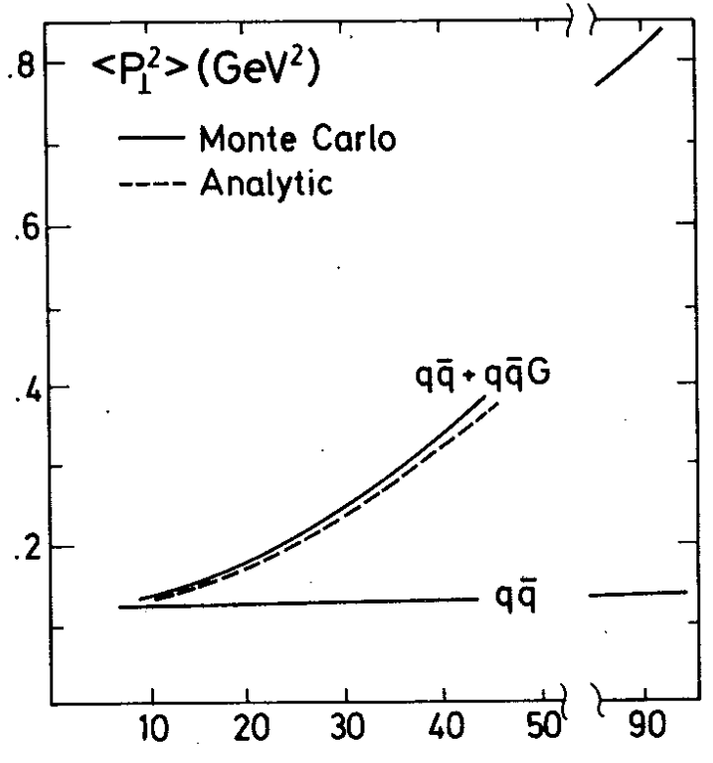

Fig. 25

We chose the $\langle p_\perp^2 \rangle$ relative to a q, $\bar{q}$ or G jet to be fixed with energy. The reason is that we believe that nonperturbative jets result from the breakup of a tube of flux of color fields with some radius $R \sim 1/\langle p_\perp \rangle$. The radius is independent of the parton energy in first approximation. Thus, so is $\langle p_\perp \rangle$ or $\langle p_\perp^2 \rangle$. This can be easily checked, since the $\langle p_\perp^2 \rangle$ increase in Fig. (25) is confined to the $q\bar{q}G$ plane. $\langle p_\perp^2 \rangle$ perpendicular to this plane ought not to grow with E to this order in α_s. (And, in fact, it does not.)

The next calculation was of the asymmetry of thin and fat jets. The jet along the thrust axis is thin because it comes from one quantum - q, $\bar{q}$ or G. The opposite jet is broad, as it comes (mostly) from q+G or $\bar{q}$+G and (seldom) from $q+\bar{q}$. This broad jet is actually two jets, which sometimes overlap. Fig. 26 shows a plot of $p_T^2(z)$ (the mean p_T^2 of a hadron with $z = p_{HAD}/E_B$.) Hadrons with $z \gtrsim 1/2$ follow a parton, and there is a clear broadening at E = 30 GeV. Again, the solid line is the Monte Carlo, and the dashed are the analytic results.

We can clearly calculate these quantities (and, if necessary, others) analytically, without a Monte Carlo model. On the other hand, such a model is of great use to experimentalists. And we see that it can be used to deliver predictions which ought to be good to 10 or 20 percent. It is important to realize that within this accuracy the predictions are model independent. They can be used as quantitative tests of QCD. A final result (from the Monte Carlo alone) is the energy flow (Fig. 27).[4]

One might ask why we calculated quadratic quantities such as $\langle p_\perp^2 \rangle$ rather than linear ones, such as $\langle p_\perp \rangle$. Asymptotically, the latter ought to be more

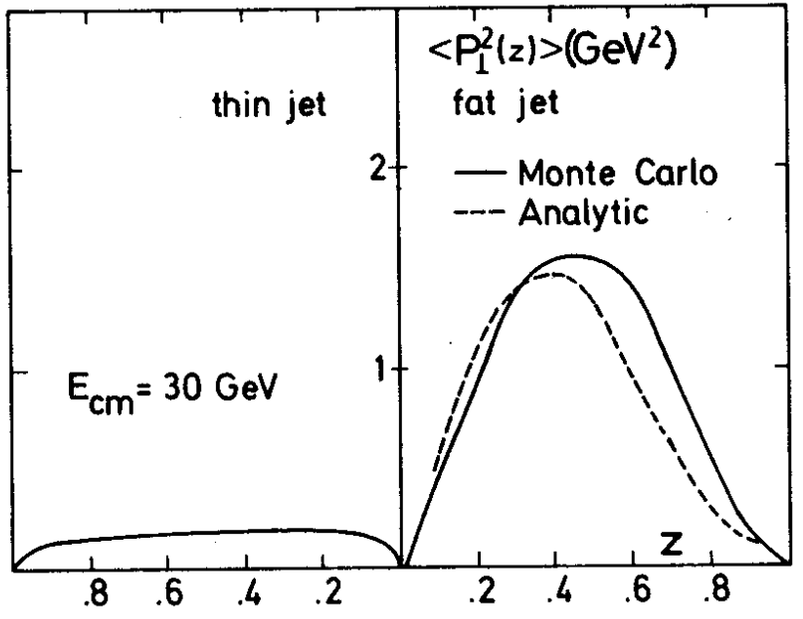
thin jet
fat jet
$\langle P_T^2(z)\rangle$(GeV^2)
Monte Carlo
Analytic
E_{cm}= 30 GeV
2
1
.8 .6 .4 .2
.2 .4 .6 .8
z

Fig. 26

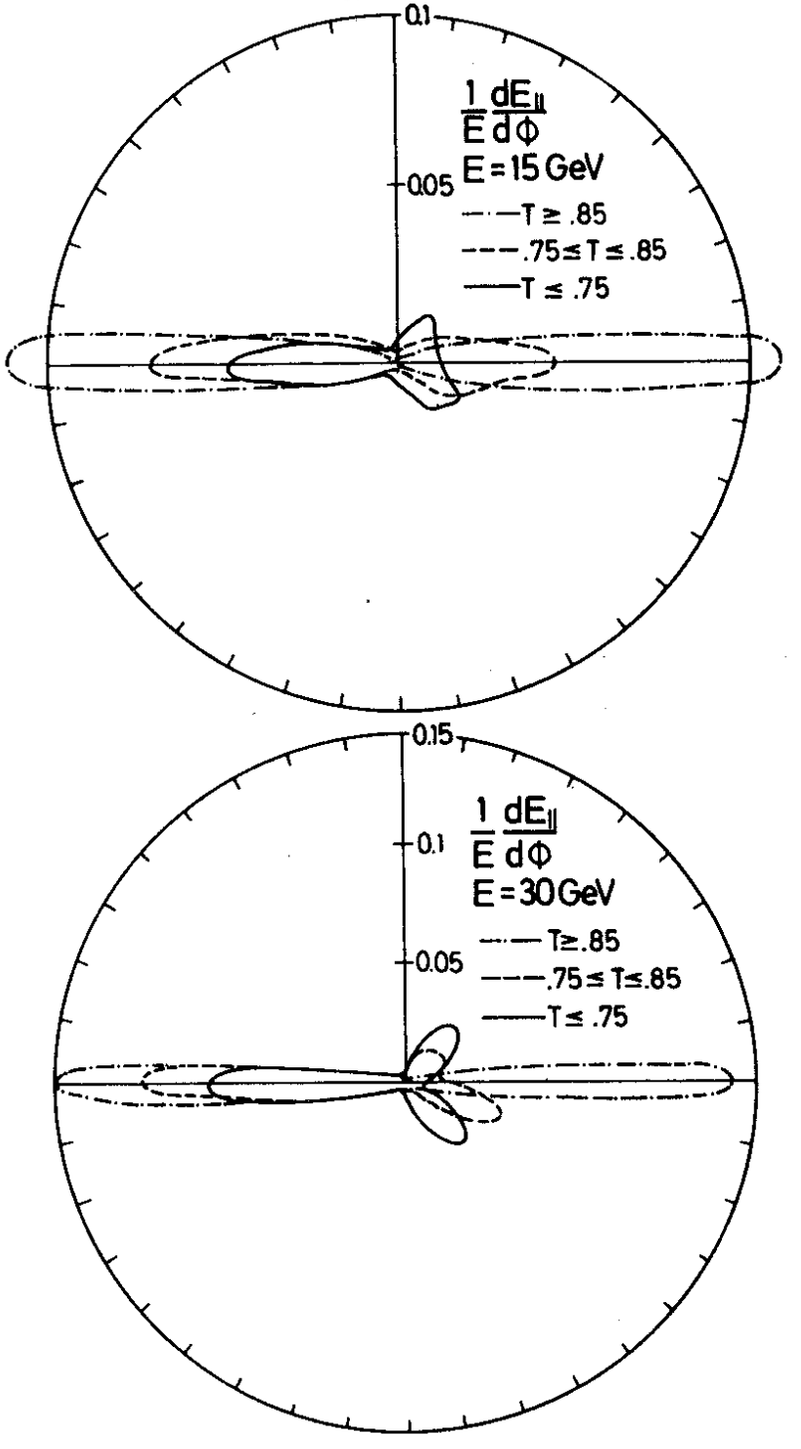
0.1
0.05
$\frac{1}{E}\frac{dE_{\parallel}}{d\Phi}$
E=15 GeV
T ≥ .85
.75≤ T ≤ .85
T ≤ .75
0.15
0.1
0.05
$\frac{1}{E}\frac{dE_{\parallel}}{d\Phi}$
E=30 GeV
T≥.85
.75≤ T≤.85
T≤ .75

Fig. 27

model-independent, just as thrust was when compared to sphericity.[23] Unfortunately, linear quantities can be more affected by nonperturbative jet development at any but asymptotic energies. Take $\langle p_T^2 \rangle$ and $\langle p_T \rangle$ as an example. They involve integrals like

$$\int dx_q\, dx_{\bar{q}}\, \frac{x_q^2 + x_{\bar{q}}^2}{(1-x_q)(1-x_{\bar{q}})} \begin{cases} \sin^2\theta_{qG} & \text{for } \langle p_\perp^2 \rangle \\ \sin\theta_{qG} & \text{for } \langle p_\perp \rangle \end{cases}$$

$$\sim \int dx_q\, dx_{\bar{q}}\, \frac{x_q^2 + x_{\bar{q}}^2}{(1-x_q)(1-x_{\bar{q}})} \begin{cases} (1-x_q)(1-x_{\bar{q}})(1-x_G)/x_q\, x_G \\ [(1-x_q)(1-x_{\bar{q}})(1-x_G)/x_q\, x_G]^{1/2} \end{cases} \qquad (21)$$

The latter $\langle p_\perp \rangle$ integral contains an integrable singularity as $T \to 1$.[24] The dependence on T_o for such a linear quantity will be stronger than for a quadratic one such as $\langle p_\perp^2 \rangle$. (Notice that both are "infrared safe" in the sense that the contribution of the collinear configuration to the integral is finite.) Since we can calculate such quadratic quantities up to the same Q (10 %) uncertainty as fixed by (unknown) corrections of higher order in α_s, there is no good reason not to do so.

Figures (28), (29) and (30) compare these results to data.[25] (In all cases, the comparison uses the Monte Carlo; but we know that it is quantitatively reliable from our comparisons to the analytic results.) Some comparisons depend on features which only the Monte Carlo can reproduce - for example the effect of having to choose a jet axis on the PLUTO data in Fig. 28), or the effect of detector resolution in the MARK J data shown in Fig. (29).

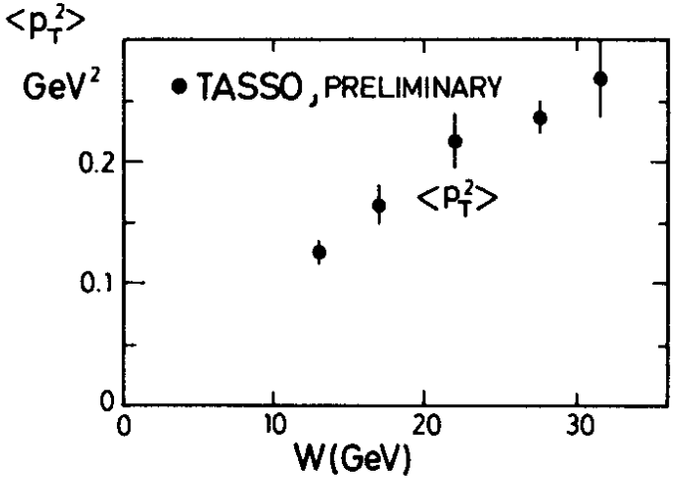

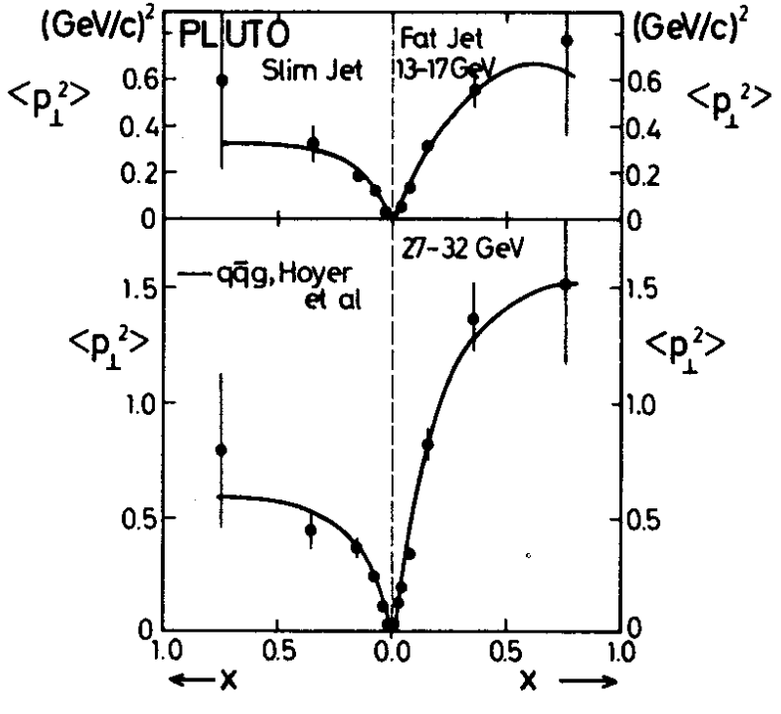

Fig. 28

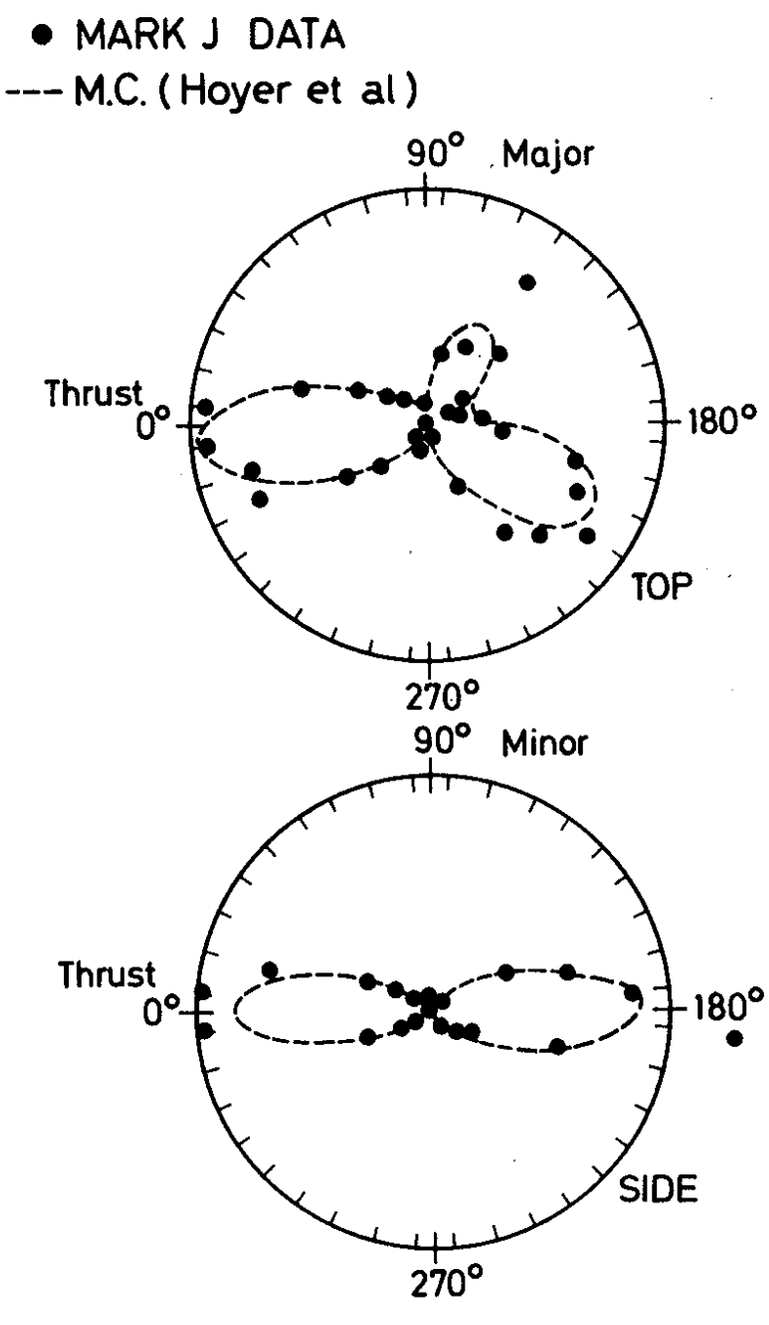
● MARK J DATA
--- M.C. (Hoyer et al)
90° Major
Thrust
0°
180°
TOP
270°
90° Minor
Thrust
0°
180°
SIDE
270°

Fig. 29

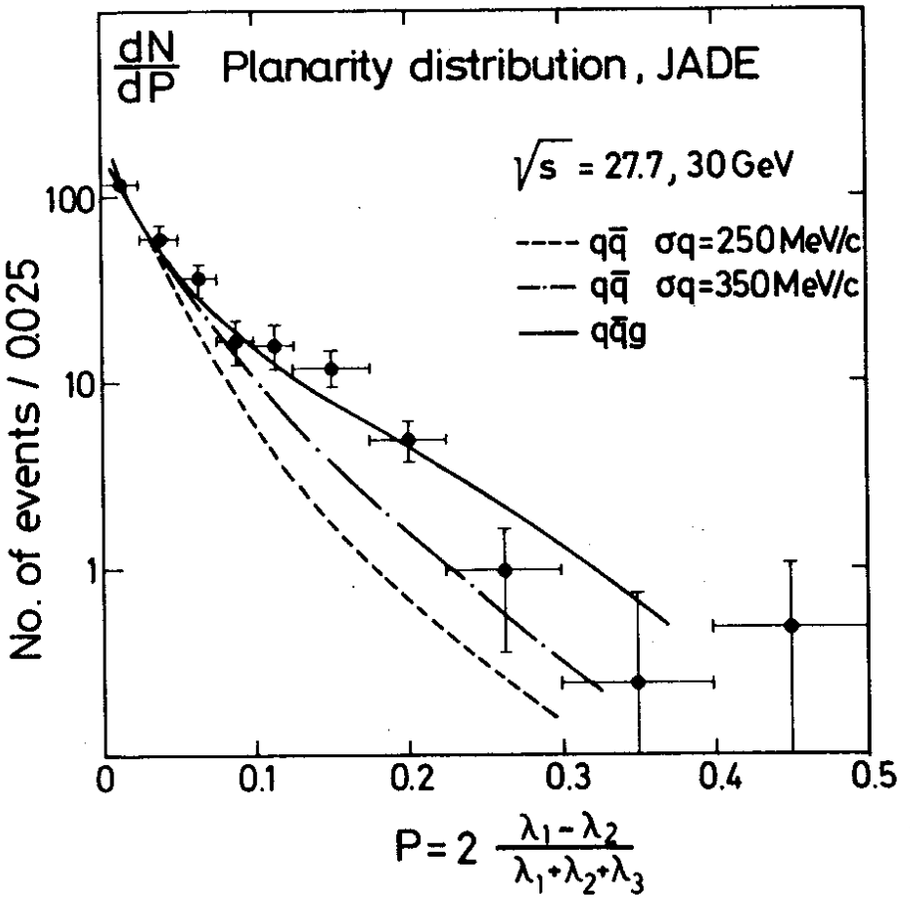
dN/dP Planarity distribution, JADE
√s = 27.7, 30 GeV
---- qq̄ σq=250 MeV/c
—·— qq̄ σq=350 MeV/c
—— qq̄g
No. of events / 0.025
100
10
1
0
0.1
0.2
0.3
0.4
0.5
P = 2 (λ1 - λ2)/(λ1+λ2+λ3)

Fig. 30

The calculations agree pretty well with the data. The agreement can hardly be better than the advertised O(10 %). Remember, these are predictions which preceeded the experimental results. They are not fits to the data.[26]

The most important feature is the appearance of well resolved three jet events. Fig. (31) shows the first TASSO 3-jet events (from P. Söding's talk at the Geneva EPS Conference last year.) Each jet clearly contains many charged particles. On the one hand, this indicates that there are three multiparticle jets - not two jets and a low multiplicity cluster instead of a third jet. It is also clear that there is no very dramatic difference between quark and gluon jets, once one accepts that the three jets are due to $e^+e^- \to q\bar{q}G$.

It is important to check that the three jets are due to the radiation of a vector quantum (the gluon). This follows by measuring angular distributions.[27] Consider the simplest of these, the angular distribution of the thrust axis relative to the beam. (Other angular asymmetries are discussed in the literature.) This is of the form $d\sigma/d\cos\theta_T \propto 1 + \alpha(T)\cos^2\theta_T$. A perturbative calculation of $\alpha(T)$ (i.e. for the partons), is shown in Fig. 32.[28] The solid line is for vector gluons. To show that agreement with QCD is nontrivial, the dashed line was calculated for scalar gluons. It is different, though not so dramatically so as for quarkonium decays, $Q\bar{Q} \to 3G \to 3$ jets.

To get an idea how much the width of quark and gluon jets affects this gluon spin test, the following table shows $\alpha(T)$ including Field-Feynman q, $\bar{q}$, G fragmentation[28]

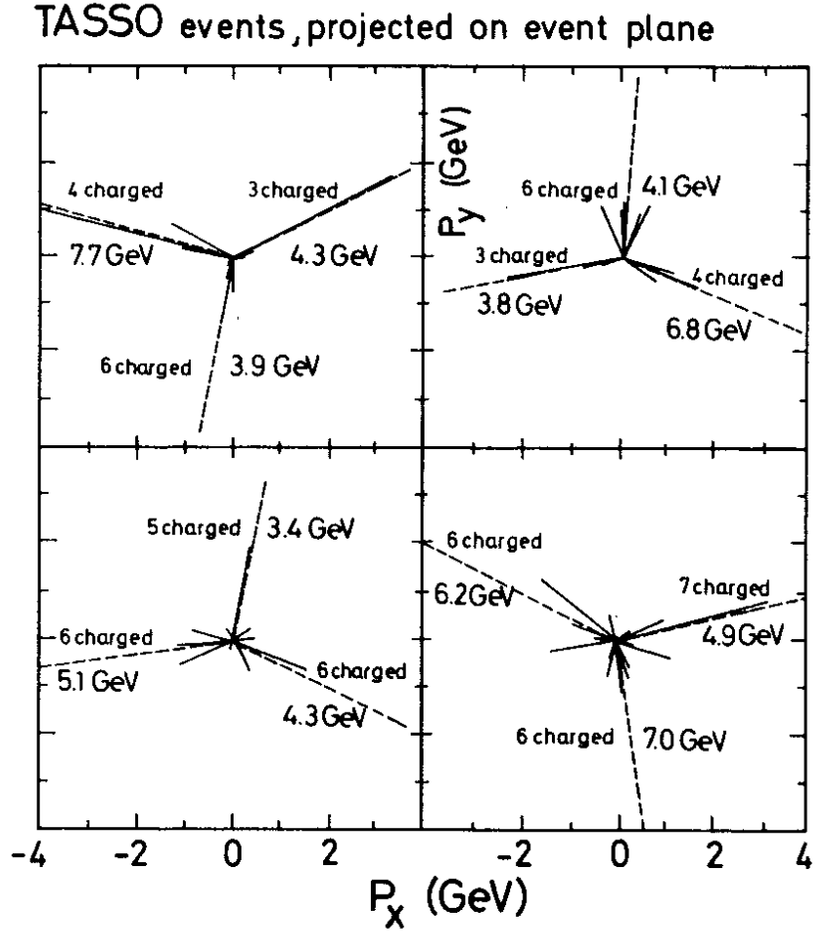

Fig. 31

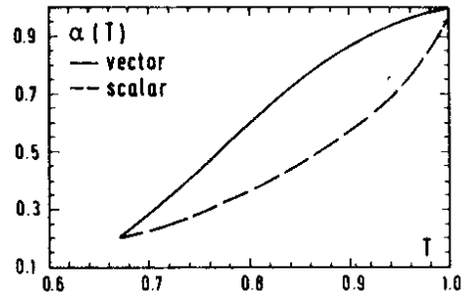

Fig. 32

	$1/2 \leq T \leq 0.7$	$.7 \leq T \leq .8$	$.8 \leq T \leq .9$
$\alpha(T)_{QCD}$	.45	.67	.94
$\alpha(T)_{SCALAR}$	.38	.48	.79

We would also like to know that one of the three jets is flavorless (no net charge, isospin, etc.). There are certainly many ways of checking this. One is to order the three jets by decreasing energy, $E_1 \geq E_2 \geq E_3$. Then form the charge correlation[19]

$$C_{12}(T) = \langle Q_1^p Q_2^p \rangle \equiv \left\langle \sum_{\text{jet 1}} e_i \left(\frac{E_i}{E_1}\right)^p \sum_{\text{jet 2}} e_j \left(\frac{E_j}{E_2}\right)^p \right\rangle \qquad (22)$$

This checks that jets 1 and 2 are q and $\bar{q}$ (ignoring the small scaling violations inside the 3 jets). C(T) is normalized at T = 1 by $e^+e^- \to q\bar{q}$. Fig. 33 shows $C_{12}(T)/C_{12}(1)$ from $e^+e^- \to q\bar{q} + q\bar{q}G$. $C_{12}(2/3)/C_{12}(1) = 1/3$

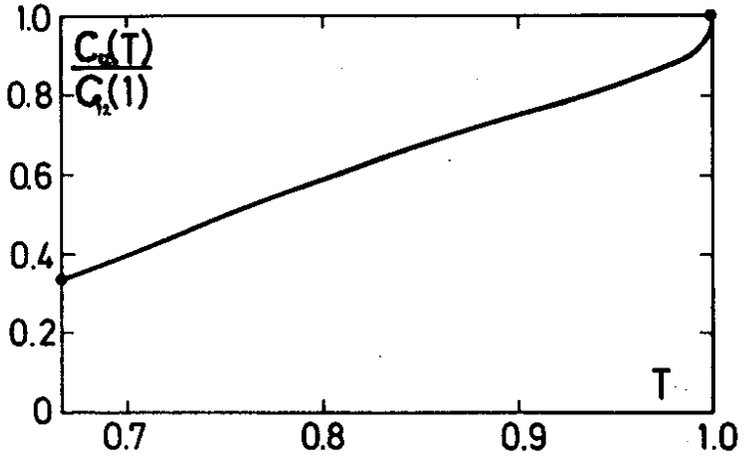

Fig. 33

because the G jet is neutral. If it were not, $C_{12}(2/3)/C_{12}(1) \neq 1/3$. (Of course, one can also measure C_{13} or C_{23}, but the third jet is less well-defined than the other two. We expect that C_{23} will be near zero, because one of these jets is often due to a (neutral) gluon.)

III. Model of a Nonperturbative Gluon Jet

One of the jets in a PETRA three-jet event is made by a gluon. Since gluons are flavor neutral, so are gluon jets.

It is a rather depressing thought that gluon jets might be undistinguished,

apart from their flavor neutrality. Since QCD is not solved, it is certainly possible that gluon jets contain hadrons with bounded $p_\perp$, uninterestingly distributed with respect to flavor and longitudinal momentum along the jet axis. Is anything more entertaining and instructive possible? It seems so. Let us construct a model of a gluon jet, paralleling the quark jet pictuce as much as possible. We start by describing a quark jet, in $e^+e^- \to q\bar{q}$. After creation, the $q\bar{q}$ rapidly separate. At distances $L \gtrsim \Lambda^{-1}$ strong color fields exist. These break up by $q\bar{q}$ pair creation. After a long time one has relativistic color neutral systems, each consisting of $q\bar{q}$ and some glue, filling up the rapidity interval between the initial q and $\bar{q}$. In its rest frame each of these color neutral systems is usually taken to be a ground state ^1S_o or ^3S_o $\bar{q}q$ meson.

A gluon jet then plausibly develops as follows.[29] In, e.g. $Q\bar{Q} \to GG$, a gluon pair is created. They separate rapidly and at distances $L \gtrsim \Lambda^{-1}$, strong color fields come into being. These break up by pair creation. But now the color charge of the gluon can only be screened by creation of color octet pairs. So a sequence of color singlet systems is formed, consisting of GG and some color flux. Inside these, more pairs can be created. If $q\bar{q}$ are made inside such a gluonic system, a flavorless ^1S_o or ^3S_o $q\bar{q}$ meson results. If more glue is made, the resulting hadron is a bound glue meson. (Thus gluon jets are ideal places to look for them.) A picture of a quark jet, and a gluon jet is shown in Fig. 34.

(In Fig. 34 the leading meson is the one to the right; less energetic ones are ordered leftward).

All this is conjecture. Even if one accepts it, there are many unclear points.

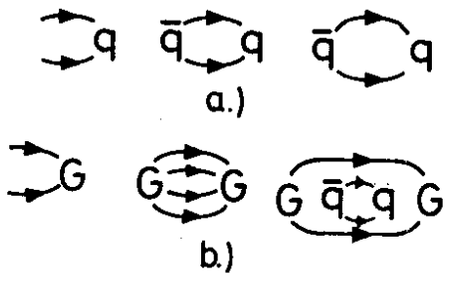

Fig. 34

First, the strict isoscalar character of the clusters may get destroyed at low momentum. Low momentum particles are probably unaware of any parent parton flavor. Beyond this, there are a number of details which can be varied. If one changes them in an attempt to find a stable clean test of the model, the following table results for leading ($z \gtrsim .3$) hadrons.

hadron/jet	quark jet u:d:s:c 4:1:1:4	gluon jet model			
		V/P=1:1 f(z)=FF	V/P=1:1 f(z)= 1	V/P=3:1 f(z)=FF	V/P=3:1 f(z)= 1
ρ^o/jet	0.07	0.07	0.12	0.04	0.06
ω/jet	0.06	0.33	0.41	0.49	0.60
ϕ/jet	0.02	0.15	0.21	0.24	0.31
K^*/jet	0.16	0	0	0	0
η/jet	0.05	0.2	0.31	0.11	0.17
η'/jet	0.04	0.37	0.45	0.18	0.23
ω/ρ^o	0.9	4.7	3.4	12.3	10

One can vary:

1) the vector $^3S_1$ to pseudoscalar ^1S_o ratio. 1:1 and 3:1 are shown. If pseudoscalars contain both $q\bar{q}$ and glue in their wave functions, a ratio even less than 1:1 is conceivable.

2) The $p_\perp$ distribution turns out to have no effect on particle ratios. Several choices of the longitudinal momentum distribution are shown. ($f(z)$ is the so-called primordial decay function, and FF stands for the FF q-jet choice.)

3) The mix of $q\bar{q}$ mesons and bound glue states. Unfortunately, bound glue mesons have not yet been clearly identified. We left them out. If they are massive, phase space will suppress their production somewhat. So the above table may not be too unrealistic. If bound glue states decay preferentially to isoscalars, then the results will change little even when they are included. Otherwise some things will change ($K^*/\text{jet} = 0$ will obviously not survive).

The most dramatic thing about this model is the dominance of isoscalars in the jets. Specifically

1) the ω/ρ^0 ratio in a gluon jet is large, $\gtrsim 3$. By comparison, the same ratio is ~ 1 for a $u\bar{u} + c\bar{c} + d\bar{d} + s\bar{s}$ mix of jets in a 4:4:1:1 ratio. A gluon jet also has lots of η mesons.

2) The leading pseudoscalar in a gluon jet is always an η or η' meson. By contrast, π^+ is frequent in a q jet.

It is possible to check this model, and to destroy it if it is false. There are several processes one can use (in order of preference).

$Q\bar{Q} \to 3G$. On a $Q\bar{Q}$ resonance, one ought to see lots of isoscalars. Off resonance, one has the standard $e^+e^- \to q\bar{q}$ jets for comparison. (Also, $Q\bar{Q} \to 3G \to$ hadrons decays are an ideal place to look for bound glue mesons.)

$e^+e^- \to q\bar{q}G$. Most of the time the thrust axis is a q or $\bar{q}$ jet. The broad jet opposite is $\bar{q}$ + G or q + G. Boosted into its rest frame, the broad jet is resolved into back-to-back jets. These are mostly qG and $\bar{q}$G jets. One can look at correlations between them, and compare these correlations to $e^+e^- \to q\bar{q} \to$ 2 jets at the same parton-parton CM energy. For example, at high particle momenta in opposite jets, qG or $\bar{q}$G will lead to predominant $\pi\eta$ correlations ($\pi\pi$ will be suppressed). $e^+e^- \to q\bar{q}$ will have $\pi\pi$ correlations stronger than $\pi\eta$ (numerically, by about a factor 2).

$qG \to qG$, $GG \to GG$, $q\bar{q} \to GG$ (in pp or $p\bar{p}$ collisions)

Presumably there are a lot of gluon jets made at large $p_\perp$ in hadron-hadron collisions. Unfortunately, almost everything here is very model dependent.

In the three cases one may also look profitably in invariant mass plots for bound glue states ζ via gluon jet fragmentation

$$G \to \zeta + \ldots$$
$$\zeta \searrow \text{identifiable hadrons}$$

IV. Multijets in QCD

It has become clear by now that the elementary quarks and gluons of QCD are "visible" via their jets at PETRA/PEP energies. (Of course, important checks such as the gluon spin in $q\bar{q}G$ remain to be done.) What will happen to a low energy jet at very high energies? Firstly, it is clear that $e^+e^- \to q\bar{q}G$ with fixed angles between all three jets is asymptotically unimportant. It vanishes

as $\sim 1/\ln Q^2$. (It is important at PETRA and PEP energies because jets have become thin enough to permit resolving a third jet.) Asymptotically, all activity in the final state is confined to some small angle about the principal jet axis. In this small angle regime, the number of resolved jets will <u>increase</u> as the energy goes up. This can be seen as follows. The rate for radiation of a gluon into an energy and angular interval E to E + dE and θ to $\theta + d\theta$ is

$$\propto \alpha_s(E_{JET}\theta)\ \frac{d\theta}{\theta}\ \frac{dE}{E} \qquad (22)$$

where E_J is the total jet energy. A gluon will be resolved as a jet if E is above some finite fraction of E_J, $E \gtrsim \epsilon E_J$ and if θ is not too small. A confinement gluon jet has angle $\theta_{NP} \sim \langle p_\perp \rangle / E$, so the total rate from (22) is $\propto \ln \ln E_J$. This becomes large. This means that on average many resolvable gluon jets will be radiated. Said differently, the number of partons at short distances proliferates slowly with E_J (provided the distances involved are really small as E_J becomes large). The partons are well separated in phase space, so that the number of visible jets inside the angular spread of a PETRA or PEP jet increases with $E_J = \sqrt{Q^2}/2$. The same applies to high p_T jets, $E_J = (p_T)_{jet}$, in pp or $p\bar{p}$ collisions.

Pictorially, this can be represented as in Fig. 35. The leftmost picture represents a moderate energy jet seen end on (E_o = 10 GeV, say). On increasing E the same (or a slightly smaller) angular range contains two resolved subjects. Increasing E further leads to more resolved subjects.[30]

Now we want to see a bit more in detail how this works for QCD.

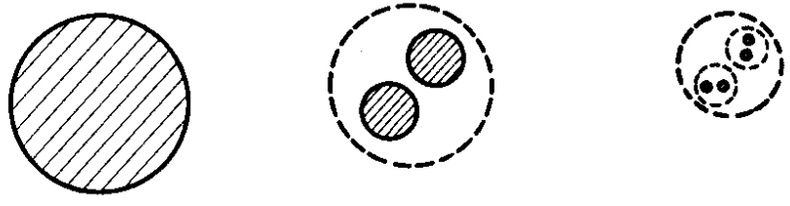

Fig. 35

<u>Confinement.</u> Since we want to use a perturbative picture of jet evolution, we need to judge when perturbation theory makes sense. We use the parton virtual mass $\sqrt{p^2}$ in investigating this. If a parton travels a short distance before it breaks up perturbatively (i.e. $q(p) \rightarrow q + G$), then the perturbative calculation is consistent. If it travels a long way, $L \gtrsim \Lambda^{-1}$, then a perturbative calculation may be doubtful. We already estimated the lab range of a parton of virtual mass $\sqrt{p^2}$ in e^+e^-,

$$L \sim E_B / p^2 \qquad (23)$$

Confinement is important for $L \gtrsim \Lambda^{-1}$ or for $p^2 \lesssim E_B\Lambda = p_c^2$. Plainly, if E_B is enormous, p_c^2 is large and it seems that perturbation theory will be bad for any parton with (large!) $p^2 \lesssim p_c^2$. However, things are not so bad. An energetic parton of mass $\sqrt{p^2}$ and energy E_B feels confining forces. After travelling a distance $\gtrsim \Lambda^{-1}$ these forces become strong enough to create a real $q\bar{q}$ pair. On travelling further, the heavy virtual partons creates many

$q\bar{q}$ pairs behind it. Color is never spread over distances larger than $O(\Lambda^{-1})$ or O(fermi). Although energy and momentum fluctuate into and out of the field attached to the heavy parton, it looses little energy and momentum to this soft $q\bar{q}$ creation process. (Eventually, of course a string of mesons are created behind the heavy virtual parton. See Fig. 36 for a leading q.)

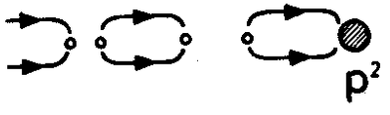

Fig. 36

We take over an estimate for the energy lost by the heavy parton from Ref. (31). (This result is for heavy partons with long life times. It should be acceptable here.) The fractional energy loss of the parton of energy E_p is

$$\frac{\Delta E_p}{E_p} = 1 - z_p \sim \frac{\text{FEW GEV}}{\sqrt{p^2}} \qquad (24)$$

We will see that as $E_p \to \infty$, so does the parton mass $\sqrt{p^2}$. So confinement will be a negligible correction (in the sense that $\Delta E_p/E_p \to 0$) - despite the fact that partons travel distances much larger than fermi! Confinement will not stop the perturbative branching. It only acts to prevent color separation

by large distances. The leading heavy parton is just dogged closely by one antiparton after another which act to balance its color. Note that the time scale to create these color screening $q\bar{q}$ pairs is shorter than the (laboratory) perturbative lifetime against $q(p) \to qG$. This is because of the time dilatation effect on q(p). (All this obviously also applies to a highly virtual gluon.)

We now go on to consider the perturbative evolution of a highly virtual and energetic quark. We use lowest order probabilities throughout, and ignore further the difference of the quark and gluon color charge. A more careful treatment can be found in ref. (32).

Hard Jets. One side of the partons giving an $e^+e^- \to$ 2 jet event is shown in Fig. 37. We imagine that this takes place at some really enormous CM energy.

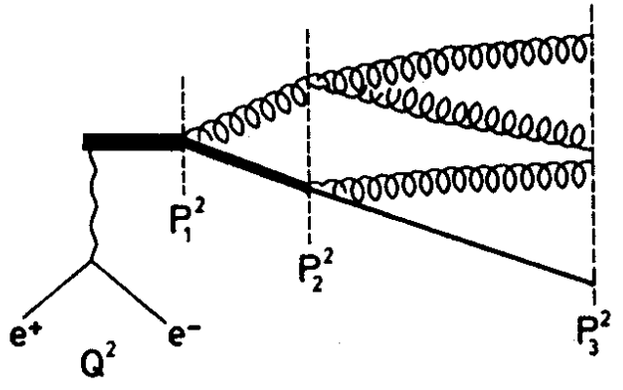

Fig. 37

The spray of partons shown is then inside some small angular range. The p_i^2 label the virtual mass at which a parton on average breaks up into two partons. In this section we suppose that each of the decay products has more than some minimum fraction z_o of the parent energy or momentum. (We will see that

$p^2 \ll E^2_{parton}$).

Now we imagine looking at some very small region, of dimensions $O(1/\sqrt{Q^2})$. Because of asymptotic freedom we see a single q(p) with $p^2 \sim O(Q^2)$. Look in a larger region, of dimension $O(1/\sqrt{p^2})$ where p^2 is larger than Q^2 but not too much larger. Then there is a <u>small</u> probability to find not a q, but q + G. This probability is small because of asymptotic freedom. Now we choose a p_1^2 (distances $\sim 1/\sqrt{p_1^2}$) such that this probability is O(1). This fixes the average invariant mass at which the first parton breakup $q(p_1) \to qG$ takes place. The daughters q and G are also off the mass shell. So there will be some average p_2^2 at which they too break up. And so on.

We use the lowest order bremsstrahlung decay formula, with p^2 in units Λ^2. Note that α_s is a function of the small distance $1/\sqrt{p^2}$. We have

$$\mathcal{P} = \int d\mathcal{P} \simeq \int_{p_1^2}^{Q^2} \frac{4\alpha_s(p^2)}{3\pi} \frac{dp^2}{p^2} \int_{z_0}^{1} \frac{dz_G}{z_G}$$

$$\simeq \beta \ln \frac{1}{z_0} \ln \left[\ln Q^2 / \ln p_1^2 \right] \qquad (25)$$

$$\sim O(1)$$

As we said, this fixes p_1^2. One might worry about using the lowest order formula. Maybe we should choose not O(1) but O(.3) or some other smaller number. Actually we are developing a semiquantitative picture, so $P \sim O(1)$ is good enough. (If one does all this more carefully, it turns out that propagation beyond $p^2 \sim O(p_1^2)$ is exponentially damped in some variable.) Now

$$p_1^2 \sim (Q^2)^{\lambda} \qquad (26)$$

where

$$\lambda \sim \exp\left[- \mathcal{P} / \beta \ln 1/z_0 \right] \sim .6 - .8$$

Since all this is self-similar, we repeat the calculation in the "rest frame" of the parton p_1. Then the ratio of successive p_k^2's at successive stages in Fig. 37 is, from (26),

$$p_{k+1}^2 / p_k^2 \sim \exp\left[- (1-\lambda) \ln p_k^2 \right] \qquad (27)$$

These ratios are very large at first, but get smaller as one goes further along the chain of breakups. Nevertheless, each p_{k+1}^2 is always much smaller than its predecessor p_k^2.

We estimate the lab range before such a hard breakup by including the Lorentz boost factor. If z_o is not too small, the momentum splits roughly evenly at each breakup. So the Lorentz boost (time dilatation) factor is of order $(1/2^k)(Q = 2E_B)$ (in units Λ again, for $p^2 \ll Q^2$). Then the range at stage k is

$$L_k \sim \frac{1}{2^k} Q^{1-2\lambda^k} \qquad (28)$$

For k = 1, $L_1 \to 0$ as $Q \to \infty$. However, for some k_c, $L_{k_c} \to \infty$ as $Q \to \infty$. The lab range diverges! We have checked that confinement is only a small

correction to these perturbative breakups. (If that were not so, we could have stopped here.) Remember that the fractional energy loss to confinement is only $\langle \Delta E_p / E_p \rangle \sim O(1/\sqrt{p^2}) \sim O(1/E^{\lambda k}) \to 0$

The ratio of successive lab angles of partons (Fig. 38) is

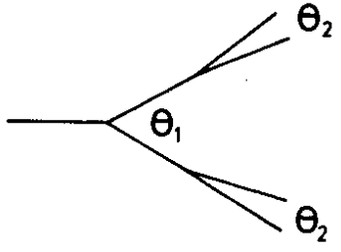

Fig. 38

$$\theta_1 \sim \sqrt{p_1^2}/Q$$
$$\theta_2/\theta_1 \sim \sqrt{p_2^2}/\sqrt{p_1^2} \sim Q^{-\lambda(1-\lambda)} \to 0 \qquad (29)$$

This means that we do have a picture where the angular spread of a low energy jet is "resolved" into subjets at high energy, and where their angular spread is found to contain further subjets at still higher energy. This is because the cone of perturbative breakup is small compared to the preceeding opening angle. It does not obscure the preceeding resolved jets. Self similarity insures that this holds for each of these partons when one increases the energy enough so they can decay into resolvable jets. (The opening angle of the energy in a confinement jet is smaller still, of order $\langle p_\perp \rangle / E_{\text{parton}}$.)

The mean number of such energetic (or calorimetrically well-defined jets

with $z_G \gtrsim z_0$) is of order

$$N_{\text{HARD JETS}} \sim (\ln Q^2)^c \qquad (30)$$

where c is some constant.

Soft Jets. All the above wantonly ignores the fact that QCD is a theory in which the gluon spectrum diverges as $1/z_G$ as the fractional momentum z_G vanishes. What does this do to the picture? Now we allow for $2p^2/Q^2 \lesssim z \lesssim 1$. (The choice $z \gtrsim 2p^2/Q^2$ just ensures that the radiated gluon goes forward with respect to the parent quark.) Now

$$P = \int dP \simeq \int_{p_1^2}^{Q^2} \frac{4\alpha_s(p^2)}{3\pi} \frac{dp^2}{p^2} \int_{2p^2/Q^2}^{1} \frac{dz_G}{z_G}$$
$$\simeq \beta \left[\ln Q^2 \ln \frac{\ln Q^2}{\ln p_1^2} - \ln \frac{Q^2}{p_1^2} \right] \qquad (31)$$
$$\sim O(1)$$

Using the ansatz $p_1^2 = (Q^2)^{1-\epsilon(Q^2)}$ we get[31]

$$p_{k+1}^2 / p_k^2 \sim \exp\left[- \text{const} \sqrt{\ln p_k^2} \right] \qquad (32)$$

instead of (27). Also the angle of radiation of the first (virtual) gluon and the total number of partons (including soft ones) is[33]

$$\langle \theta_1 \rangle \sim \sqrt{\ln Q^2}\, \exp\left[-\text{const}\sqrt{\ln Q^2}\right]$$

$$N_{\text{SOFT PARTONS}} \sim \exp\left[\text{const}\sqrt{\ln Q^2}\right] \qquad (33)$$

(Note that although the radiations at early times are "soft", $z \ll 1$, they are far off shell, $p^2 \gg 1$.)

Fig. 39 shows a picture of this. A hard parton which is also far off its

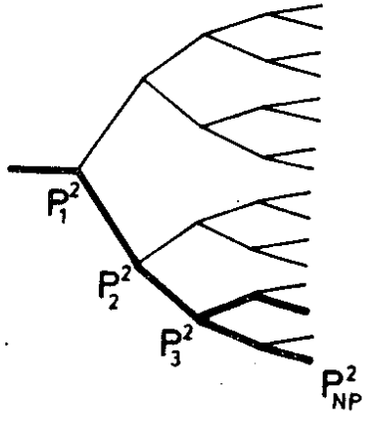

Fig. 39

mass shell migrates down in p^2 by emitting soft virtual gluons. Eventually p^2 drops by a big factor $\sim \exp(-\text{const}\ p_k^2)$ and two energetic partons result. These also bobble down in p^2 by emitting soft virtual gluons. (Because of the vector nature of gluons and the 3G vertex, they act pretty much as do quarks

in this branching process. Of course, they have a larger color charge, and the breakup probability is larger by a factor 9/4 . But it has the same dz_G/z_G spectrum at small z_G.)

The angular scale of all this is roughly as follows. The calorimetric jets (i.e. $z \geq$ some z_0) are well resolved as before. But they are accompanied at each hard breakup stage by "stragglers"-virtual gluons emitted with little fractional energy, but at large angles. Thus each hard calorimetric jet is accompanied by soft junk at larger angles, (33). The energy in this halo of partons is not large but the number of partons is large, equ. (33). By similarity, each of the subjets has such a halo.

At what p^2 should this branching stop? Clearly, at some p^2_{NP} confinement is more than a correction. We chose $p^2_{NP} = 20\ \text{GeV}^2$ (~ 80 in units Λ^2) as the place to stop the perturbative branching. By analogy to SPEAR data at $\sqrt{Q^2} = 7.4$ GeV, a $p^2_{NP} \sim 50\ \text{GeV}^2$ will give barely resolvable $q \to qG$ jets. $p^2_{NP} = 20\ \text{GeV}^2$ clearly will not, so it is a reasonable place to stop. Because of our earlier space time arguments, confinement is probably important for $p^2 < p^2_{NP} \sim 20\ \text{GeV}^2$. Perturbative evolution below this is theoretically a bit suspect.

In order to judge the importance of both confinement jets and the soft radiation, we also made a Monte Carlo model. It follows q and G branching and at $p^2 \leq p^2_{NP}$, attaches Feynman-Field jets. The individual hadron momenta in these jets are then smeared together so as to make an optically intelligible plot. Fig. 40 is particularly interesting. It shows a gluon jet at 320 GeV. It has split up into a hard gluon and a soft one. This is the dz_G/z_G behavior of gluons radiated by gluons. Observation of this effect would be transparent

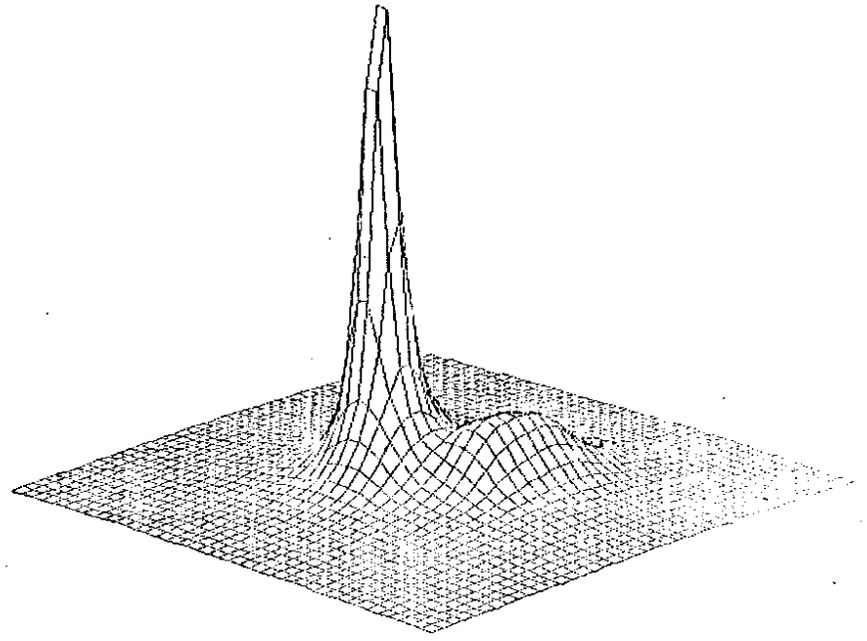

Fig. 40

G jet on a .4 x .4 radian plot

evidence that QCD really is a theory with self-coupled vector gluons. Fig. 41 shows a gluon jet at really enormous energy, 3200 GeV = 3.2 TeV. It shows the resolved jets-in-jets behavior. Finally, Fig. 42 shows a 3.2 TeV q jet with a wide angle soft gluon jet of the sort we described. So far as we can judge, this soft radiation - characteristic of QCD - does not destroy a jets-within-jets picture at high energy.

Since partons are "observable" as jets, one can speculate about what to do with them. Clearly, we have seen that the jets are well enough defined to make parton-parton (or 3 parton) invariant mass plots. Bjorken pointed out some time ago that a really massive quark (M_t 30 GeV) might be observed via a three jet decay,

$$t \rightarrow q\bar{q}q \rightarrow 3 \text{ jets} \tag{34}$$

Also, a massive neutral Higgs boson (M_H 100-200 GeV) might be seen via

$$H \rightarrow t\bar{t} \begin{cases} \rightarrow \bar{q}\bar{q}q \rightarrow 3 \text{ jets} \\ \rightarrow q\bar{q}q \rightarrow 3 \text{ jets} \end{cases} \tag{35}$$

or for $M_H > 2M_W$

$$H \rightarrow W^+W^- \rightarrow q\bar{q} + q\bar{q} \rightarrow 4 \text{ Jets} \tag{36}$$

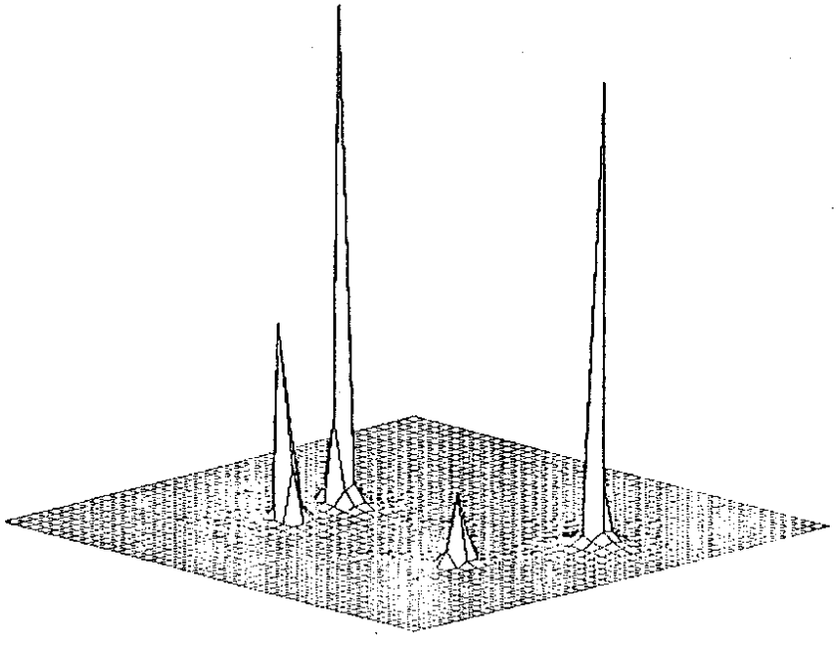

Fig. 41

G jet on a .4 x .4 radian plot

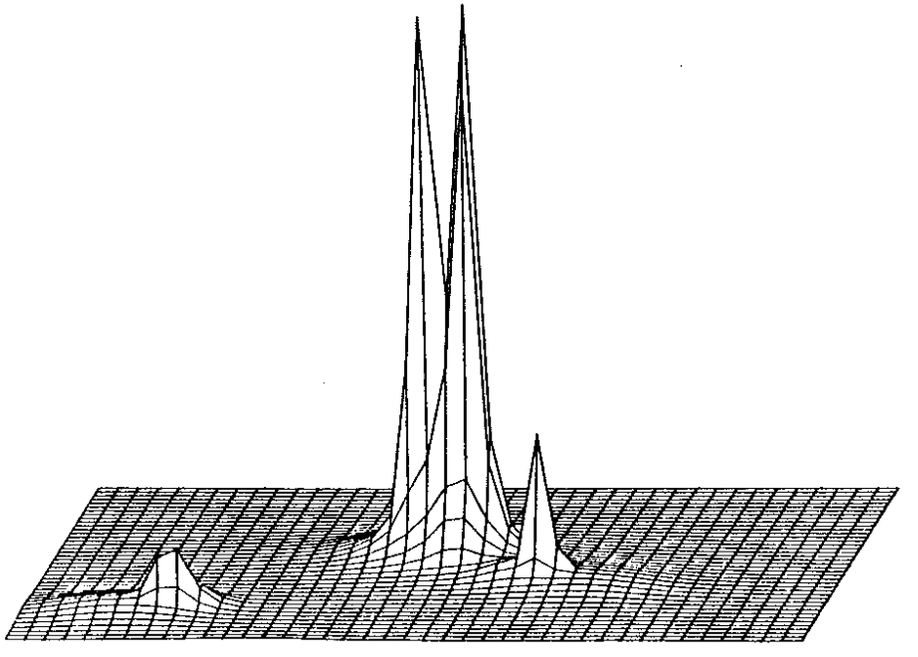

Fig. 42

q jet on a .8 x .8 radian plot

In addition, any new colored object which decays to known colored partons q and G might be seen this way

$$\text{new colored object} \rightarrow \text{quarks + gluons} \rightarrow \text{jets} \qquad (37)$$

The resolution one can achieve in such multiparton invariant masses clearly depends on the QCD smearing of the partons' virtual mass as produced in a decay like (36). This may be the most useful purpose for the considerations of this section, sometime in the distant future.

Acknowledgements

I owe particular and obvious thanks to P. Hoyer, K. Koller, H. Krasemann, C.H. Lai, P. Osland, J.L. Petersen, C. Peterson, H.G. Sander and P.M. Zerwas. I also wish to thank Prof. H. Mitter and his colleagues for organizing such a nice school.

References

1) There are numerous reviews of QCD which include references to the original literature. See H.D. Politzer, Phys. Rep. 14C (1974) 129; W. Marciano and H. Pagels, Phys. Rep. 36C (1978) 137.

2) Jet development has been analyzed by J.D. Bjorken, Current Induced Reactions, Springer 1976; F. Low and K. Gottfried, Phys. Rev. D17 (1979) 2487; B. Andersson, G. Gustafson and C. Peterson, Z. Physik C 1 (1979) 105. Our discussion roughly follows that in the first reference.

3) This proliferation is nicely described by J. Kogut and L. Susskind, Phys. Rev. D9 (1974) 697, 3391.

4) see in particular A. de Rújula, J. Ellis, M.K. Gaillard and E. Floratos, Nucl. Phys. B138 (1978) 387; for critical remarks, see S. Brandt and H.D. Dahmen, Z. Physik C 1 (1979) 61.

5) For detailed accounts of the SPEAR data, see G.G. Hanson, SLAC-Pub 1814 (September, 1976) and SLAC-Pub-2118 (May, 1978).

6) PLUTO collaboration, Phys. Lett. 78B (1978) 176.

7) O. Nachtmann, these proceedings.

8) For general discussions of quarkonium, see M. Krammer and H. Krasemann, Acta Physica Austriaca, Suppl. XXI (1979) 259 (Springer, 1979); V.A. Novikov et al., Phys. Rep. 41C (1978) 1.

9) T. Appelquist and H.D. Politzer, Phys. Rev. Lett. 34 (1975) 43; Phys. Rev. D12 (1975) 1404.

10) K. Koller and T.F. Walsh, Nucl. Phys. B140 (1978) 449 and references there. The QCD result for α_N was found by S. Brodsky et al., Phys. Lett. 73B (1978) 203.

11) There have been repeated suggestions that higher order QCD corrections to $Q\bar{Q}$ decay rates may be large. For recent work and further references, see R. Barbieri, E. d'Emilio, G. Curci and E. Remiddi, CERN preprint TH 2622 (January, 1979).

12) K. Koller and H. Krasemann, Phys. Lett. 88B (1979) 119.

13) K. Koller, H. Krasemann and T.F. Walsh, Z. Physik C 1 (1979) 71.

14) PLUTO Collaboration, presented by S. Brandt at the 1979 EPS Conference, DESY report 79/42 (1979).

15) T.F. Walsh and P.M. Zerwas, DESY preprint 80/20.

16) J. Ellis, M.K. Gaillard and G. Ross, Nucl. Phys. B111 (1976) 253.

17) A. Ali, J.G. Körner, Z. Kunszt, E. Pietarinen, G. Kramer, G. Schierholz and J. Willrodt, Phys. Lett. 82B, 285 (1979) and DESY preprint 79/54.

18) M. Dine and J. Sapirstein, Phys. Rev. Lett. 43 (1979) 668;
K.G. Chetyrkin, A.L. Kataev and F.V. Tkachov, Phys. Lett. 85B (1979) 277;
W. Celmaster and R.J. Gonsalves, Phys. Rev. Lett. 44 (1980) 560.

19) P. Hoyer, P. Osland, H.G. Sander, T.F. Walsh and P.M. Zerwas, Nucl. Phys. B161 (1979) 349.

20) Notice that above 30 GeV T_o as we chose it is large enough so that one can just resolve $q \to qG \to 2$ jets from an off-shell parton. (By analogy to SPEAR $e^+e^- \to q\bar{q} \to 2$ jets). Clearly, it would make no sense to choose T_o smaller than we did. Maybe it should be a bit larger at energies above 30 GeV.

21) The uncertainty principle might lead us to choose $1/\sqrt{p^2}$ as the "distance" at which α_s is measured. Then $\alpha_s(Q^2) \to \alpha_s((1-T)Q^2) = \alpha_s(p^2)$. Note that this is equivalent to a higher order correction in $1/\ln Q^2$.

22) B. Andersson, G. Gustafson and C. Peterson, Nucl. Phys. B135, (1978) 273;
R. Field and R.P. Feynman, Nucl. Phys. B136 (1978) 1.

23) There is a large literature on linear observables. See ref. 4 and
G.C. Fox and S. Wolfram, Nucl. Phys. B141 (1979) 413 and Z. Physik C 4 (1980) 237;
S.Y. Pi, R.L. Jaffe and F. Low, Phys. Rev. Lett. 41 (1978) 142;
C.L. Basham, L.S. Brown, S.D. Ellis and S.T. Love, Phys. Rev. D17 (1978) 2298; D19 (1979) 2018;
H. Georgi and J. Sheiman, Phys. Rev. D20 (1979) 111;
This stems from
G. Sterman and W. Weinberg, Phys. Rev. Lett. 39 (1977) 1436.

24) So does the integral for the mean value $\langle 1-T \rangle$. See ref. 4.

25) TASSO Collaboration, Phys. Lett. 86B (1979) 243;
MARK J Collaboration, Phys. Rev. Lett. 43 (1979) 830;
PLUTO Collaboration, Phys. Lett. 86B (1979) 418;
JADE Collaboration, DESY preprint 79/80 (December, 1979).

26) There now exists a more detailed Monte Carlo model by A. Ali, E. Pietarinen, G. Kramer and J. Willrodt, DESY preprint 79/86 (December, 1979) which is being used to fit data so as to extract α_s.

27) G. Kramer, G. Schierholz and J. Willrodt, Phys. Lett. 79B (1978) 249;
(E: 80B (1979) 433);
G. Schierholz, DESY report 79/71 (October, 1979).
Another independent test is due to J. Ellis and I. Karliner, Nucl. Phys. B148 (1979) 141.

28) K. Koller, H. Sander, T.F. Walsh and P.M. Zerwas, DESY preprint 79/87 (December, 1979).

29) C. Peterson and T.F. Walsh, NORDITA preprint 80/1.
A model which is quite different in motivation is that due to
B. Andersson and C. Gustafson, Z. Physik C 3 (1980) 223
where a gluon jet is treated as a kink on a confinement string joining q and $\bar{q}$.

30) The idea that field theories lead to a multijet final state is due to
A.M. Polyakov, JETP (Sov. Phys.) 32 (1971) 296; 33 (1971) 850.
This can be pictorially represented as a branching process,
S.J. Orfanidis and V. Rittenberg, Phys. Rev. D10 (1974) 2892;
P. Cvitanović, P. Hoyer and K. Konishi, Phys. Lett. 85B (1979) 413.

31) M. Suzuki, Phys. Lett. 71B (1977) 140;
J.D. Bjorken, Phys. Rev. D17 (1978) 171.

32) C.H. Lai, J.L. Peterson and T.F. Walsh, Niels Bohr Institute preprint NBI-HE-80-8. The space time picture presented here is an extension of work by
L. Caneschi and A. Schwimmer, Phys. Lett. 86B (1979) 179;
C.B. Chiu and J. Szwed, MPI preprint MPI-PAE/Pth 15/79.

33) The result for $N_{SOFT\ PARTONS}$ is due to
W. Furmanski, R. Petronzio and S. Pokorski, Nucl. Phys. B155 (1979) 253;
K. Konishi, Rutherford preprint RL-79-035 (May, 1979);
A. Bassetto, M. Ciafaloni and G. Marchesini, Phys. Lett. 86B (1979) 366.

34) J.D. Bjorken, unpublished.